Fundamentals of Magnetism II
Critical Switching curve:
Coupled vs. Uncoupled Magnetic Systems

Leonard Spinu
University of New Orleans

MAGNETIZATION SWITCHING

Magnetization changes by rotation = Switching

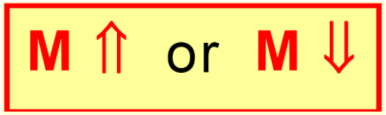

❑ Static switching – SW switching

- Stonner-Wohlfarth model
- Single domain particles
- DC applied field

Two stable states (logical "0" and "1")

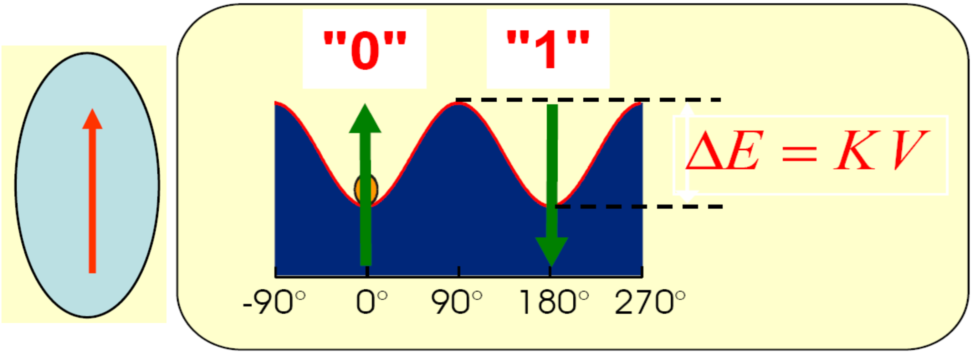

❑ Dynamic switching (control of switching field and time)

- Switching time
- M(t) – LLG equation
- H(t) (Pulsed field)

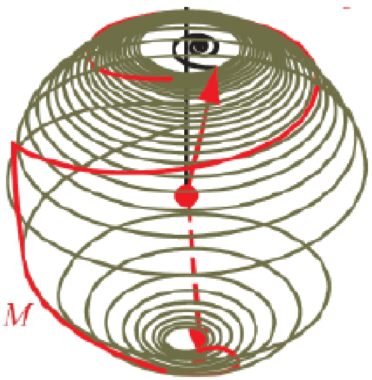

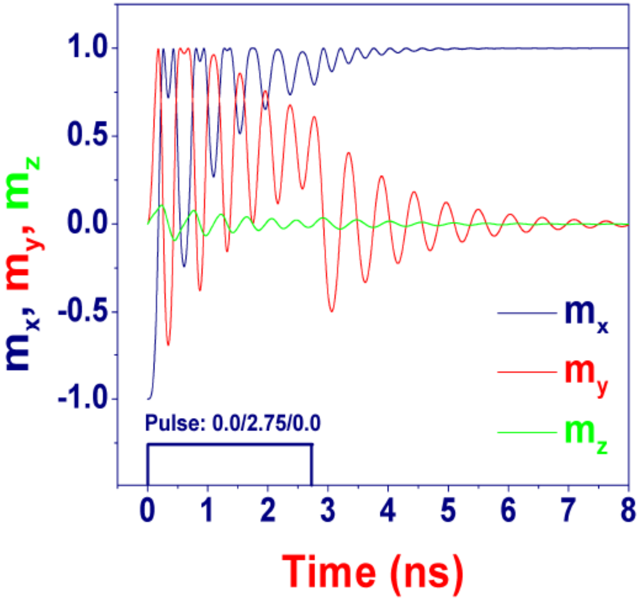

Stoner-Wohlfarth Model

- Single Domain Particles at T=0K
- No Interactions
- Uniaxial anisotropy
- Coherent Rotation
- Very useful in modeling magnetic particles in
  - Magnetic storage
  - Biomagnetism
  - Rock Magnetism
  - Paleomagnetism

Stoner-Wohlfarth Model

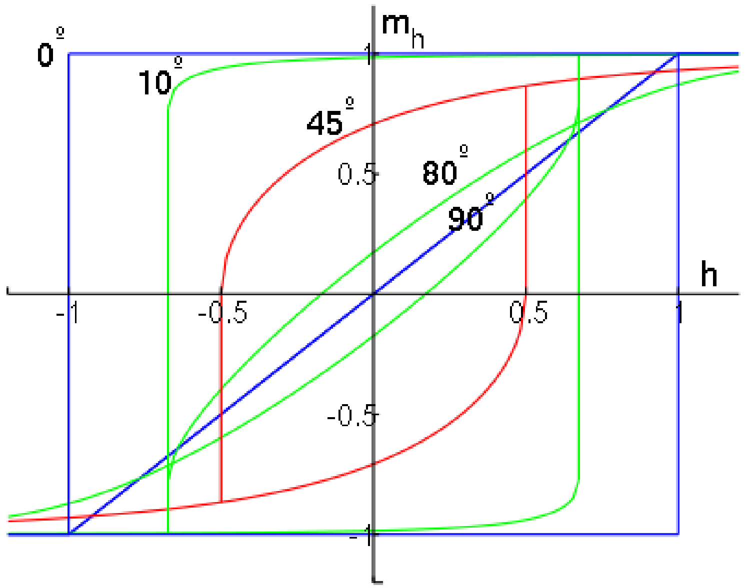

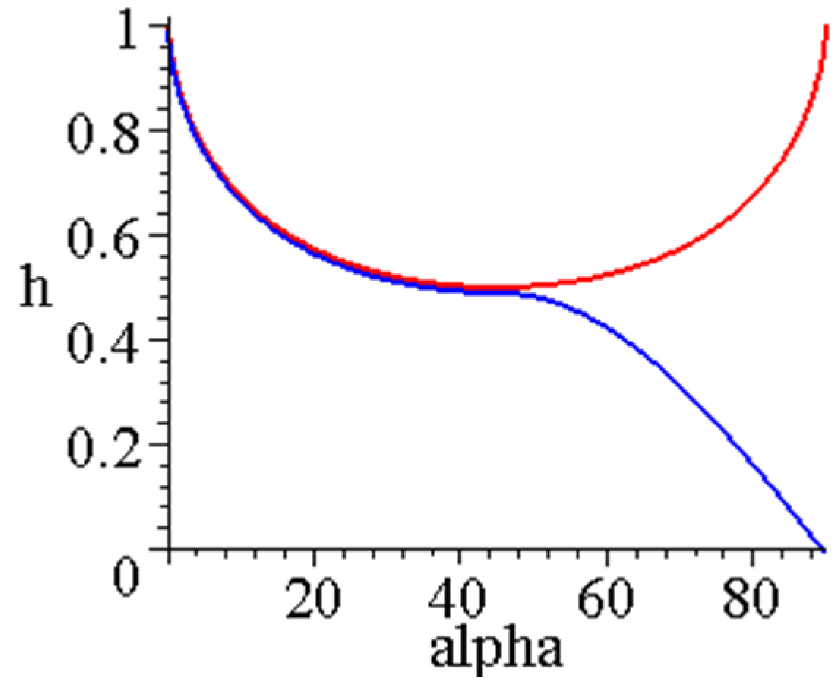

SWITCHING & CRITICAL CURVE

A MECHANISM OF MAGNETIC HYSTERESIS IN HETEROGENEOUS ALLOYS

By E. C. STONER, F.R.S. and E. P. WOHLFARTH
Physics Department, University of Leeds

(*Received* 24 *July* 1947)

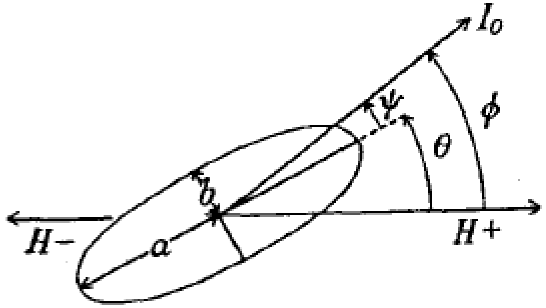

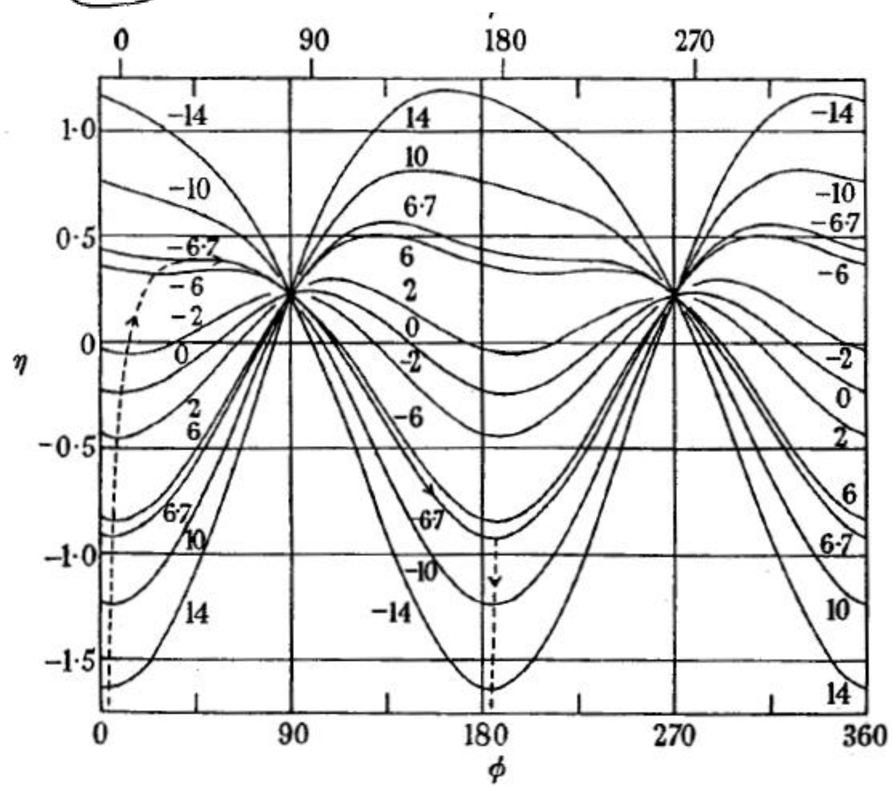

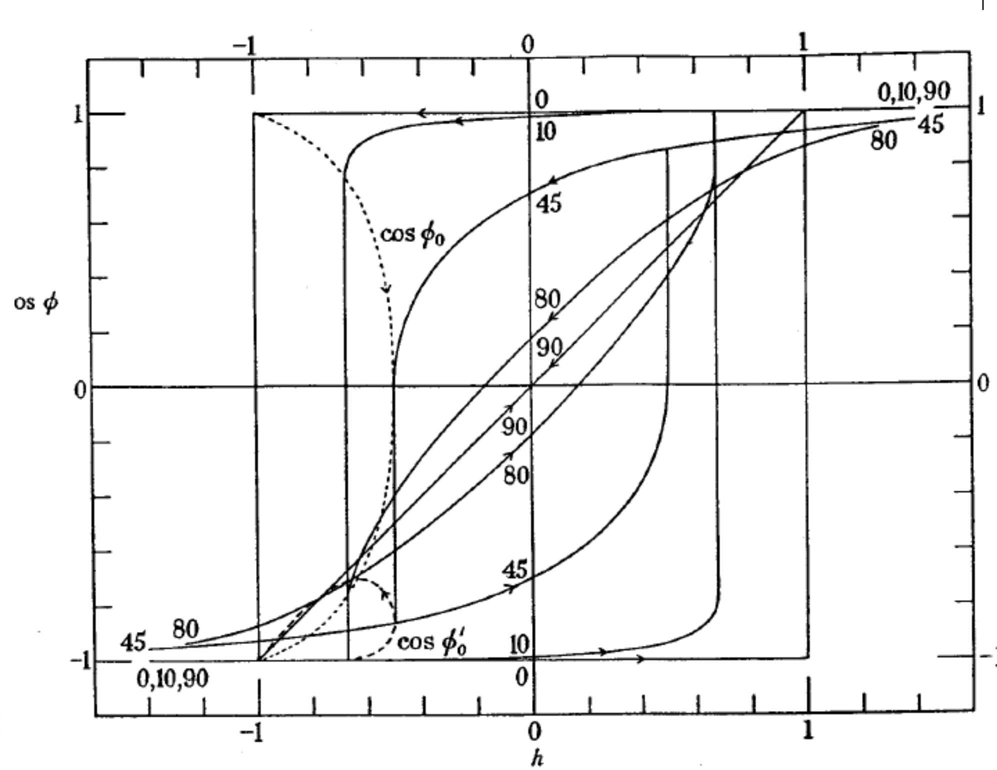

TABLE 3. DEPENDENCE OF $\cos\phi$ ON h AND θ FOR PROLATE SPHEROID

$h \backslash \theta$	10	20	30	40	45	50	60	70	80	90
2·0	0·9983	0·9935	0·9864	0·9783	0·9744	0·9712	0·9683	0·9734	0·9883	1·0
1·5	0·9975	0·9906	0·9798	0·9666	0·9598	0·9534	0·9441	0·9453	0·9676	1·0
1·4	0·9974	0·9897	0·9779	0·9632	0·9555	0·9481	0·9366	0·9356	0·9582	1·0
1·3	0·9971	0·9888	0·9757	0·9593	0·9506	0·9420	0·9277	0·9237	0·9452	1·0
1·2	0·9969	0·9877	0·9733	0·9549	0·9449	0·9349	0·9172	0·9091	0·9273	1·0
1·1	0·9966	0·9865	0·9704	0·9498	0·9383	0·9266	0·9047	0·8913	0·9031	1·0
1·0	0·9962	0·9850	0·9672	0·9438	0·9306	0·9169	0·8900	0·8697	0·8715	1·0
0·9	0·9958	0·9834	0·9633	0·9368	0·9222	0·9055	0·8726	0·8437	0·8318	0·9
0·8	0·9953	0·9814	0·9589	0·9286	0·9110	0·8921	0·8521	0·8128	0·7841	0·8
0·7	0·9947	0·9791	0·9536	0·9189	0·8985	0·8763	0·8278	0·7766	0·7286	0·7
0·6	0·9941	0·9764	0·9473	0·9074	0·8837	0·8516	0·7994	0·7345	0·6660	0·6
0·5	0·9932	0·9730	0·9397	0·8936	0·8660	0·8355	0·7660	0·6862	0·5972	0·5
0·4	0·9922	0·9690	0·9305	0·8771	0·8449	0·8092	0·7272	0·6316	0·5225	0·4
0·3	0·9910	0·9640	0·9193	0·8572	0·8197	0·7780	0·6821	0·5702	0·4427	0·3
0·2	0·9894	0·9578	0·9055	0·8329	0·7892	0·7407	0·6300	0·5018	0·3578	0·2
0·1	0·9874	0·9499	0·8881	0·8031	0·7523	0·6962	0·5697	0·4260	0·2682	0·1
0·0	0·9848	0·9397	0·8660	0·7660	0·7071	0·6428	0·5000	0·3420	0·1736	0·0
−0·1	0·9813	0·9261	0·8374	0·7194	0·6512	0·5779	0·4190	0·2490	0·0741	−0·1
−0·2	0·9764	0·9075	0·7991	0·6593	0·5807	0·4977	0·3236	0·1451	−0·0311	−0·2
−0·3	0·9692	0·8809	0·7457	0·5786	0·4880	0·3952	0·2085	0·0275	−0·1429	−0·3
−0·4	0·9583	0·8410	0·6645	0·4596	0·3551	0·2528	0·0612	−0·1103	−0·2632	−0·4
−0·5	0·9397	0·7660	0·5000	0·1736	0·0000	−0·0481	−0·1736	−0·2868	−0·3961	−0·5
−0·6	0·9015	—	—	—	—	—	—	—	−0·5542	−0·6
−0·7	—	—	—	—	—	—	—	—	—	−0·7
−0·8	—	—	—	—	—	—	—	—	—	−0·8
−0·9	—	—	—	—	—	—	—	—	—	−0·9
−1·0	—	—	—	—	—	—	—	—	—	−1·0
$\cos\phi_0$	0·7740	0·5660	0·3456	0·1162	0·0000	−0·1162	−0·3456	−0·5660	−0·7740	−1·0
$\cos\phi_0'$	−0·9946	−0·9750	−0·9416	−0·8940	−0·8660	−0·8361	−0·7745	−0·7224	−0·7128	−1·0

Table 4. Critical field, h_0, critical angle of magnetization, ϕ_0, and related quantities as dependent on orientation, θ, of prolate spheroid

ϕ_0 and ϕ_0' are the initial and final angles made by the magnetization vector, I_0, with the positive direction of the field, as h, decreasing from a positive value greater than $|h_0|$, passes through the value h_0. The resolved value of the magnetization in the positive direction of the field is given by $I_0 \cos\phi$. The jump in the resolved magnetization at h_0 is given by $I_0(\cos\phi_0' - \cos\phi_0)$.

$h = H/(N_b - N_a)\, I_0$, where N_a and N_b are the demagnetization coefficients along the polar and equatorial axes respectively.

θ	$-h_0$	ϕ_0	$\cos\phi_0$	$\phi_0' - 180$	$-\cos\phi_0'$	$\cos\phi_0' - \cos\phi_0$
0	1·00000	0·000	1·00000	0·000	1·00000	−2·00000
1	0·90707	15·542	0·96343	0·524	0·99996	−1·96339
2	0·85929	20·100	0·93919	1·076	0·99982	−1·93901
4	0·79237	26·391	0·89578	2·231	0·99924	−1·89502
6	0·74370	31·264	0·85479	3·440	0·99820	−1·85299
8	0·70531	35·471	0·81441	4·689	0·99665	−1·81106
10	0·67381	39·287	0·77404	5·971	0·99458	−1·76862
12	0·64733	42·829	0·73339	7·279	0·99194	−1·72533
14	0·62475	46·186	0·69232	8·610	0·98873	−1·68105
16	0·60527	49·402	0·65075	9·958	0·98493	−1·63568
18	0·58838	52·508	0·60865	11·322	0·98054	−1·58920
20	0·57365	55·526	0·56603	12·697	0·97555	−1·54158
30	0·52402	69·784	0·34557	19·671	0·94164	−1·28721
40	0·50255	83·326	0·11623	26·618	0·89402	−1·01025
45	0·50000	90·000	0·00000	30·000	0·86603	−0·86603
50	0·50255	96·674	−0·11623	33·269	0·83610	−0·71987
60	0·52402	110·216	−0·34557	39·238	0·77452	−0·42896
70	0·57365	124·474	−0·56603	43·749	0·72237	−0·15634
72	0·58838	127·492	−0·60865	44·337	0·71524	−0·10659
74	0·60527	130·598	−0·65075	44·762	0·71004	−0·05929
76	0·62475	133·814	−0·69232	44·982	0·70733	−0·01501
78	0·64733	137·171	−0·73339	44·936	0·70789	+0·02550
80	0·67381	140·713	−0·77404	44·534	0·71283	+0·06121
82	0·70531	144·529	−0·81441	43·630	0·72380	+0·09061
84	0·74370	148·736	−0·85479	41·968	0·74352	+0·11126
86	0·79237	153·609	−0·89578	39·013	0·77700	+0·11878
88	0·85929	159·900	−0·93919	33·277	0·83603	+0·10316
89	0·90707	164·458	−0·96343	27·609	0·88614	+0·07730
90	1·00000	180·000	−1·00000	0·000	1·00000	0·00000

SWITCHING & CRITICAL CURVE

research memorandum

IBM RESEARCH CENTER POUGHKEEPSIE, N Y

no. RM 003.111.224
date October 1, 1956

THEORY OF MAGNETIC HYSTERESIS IN
FILMS AND ITS APPLICATION TO COMPUTERS

by

J. C. SLONCZEWSKI

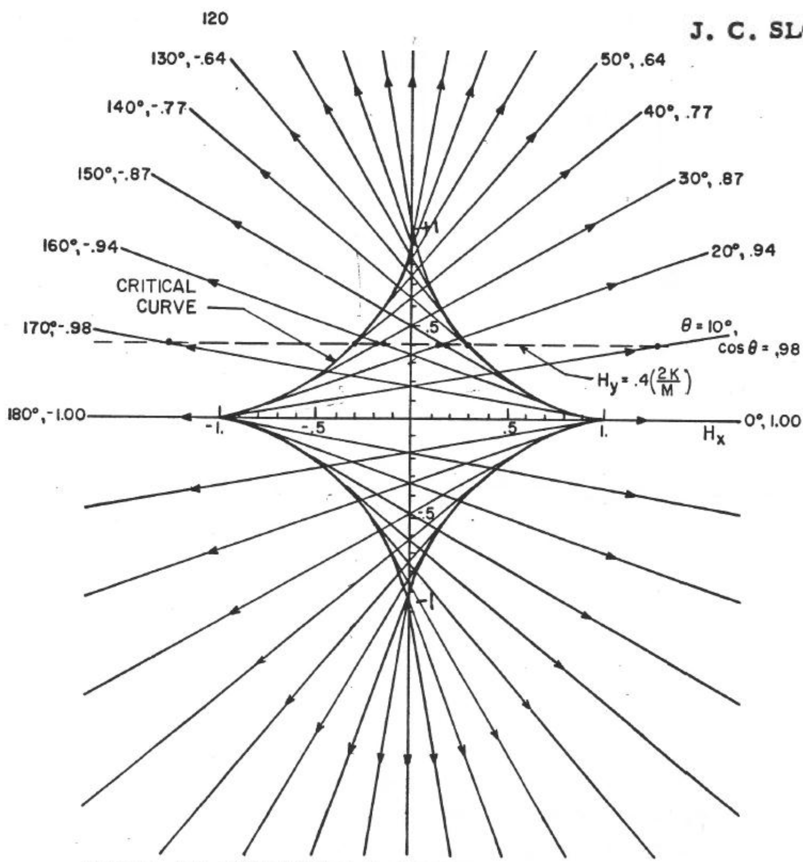

FIGURE 3. THE ORIENTATION OF M, INDICATED BY ARROWS, DEPENDS ON $\vec{H}$. H_x AND H_y ARE IN UNITS OF $\frac{2K}{M}$.

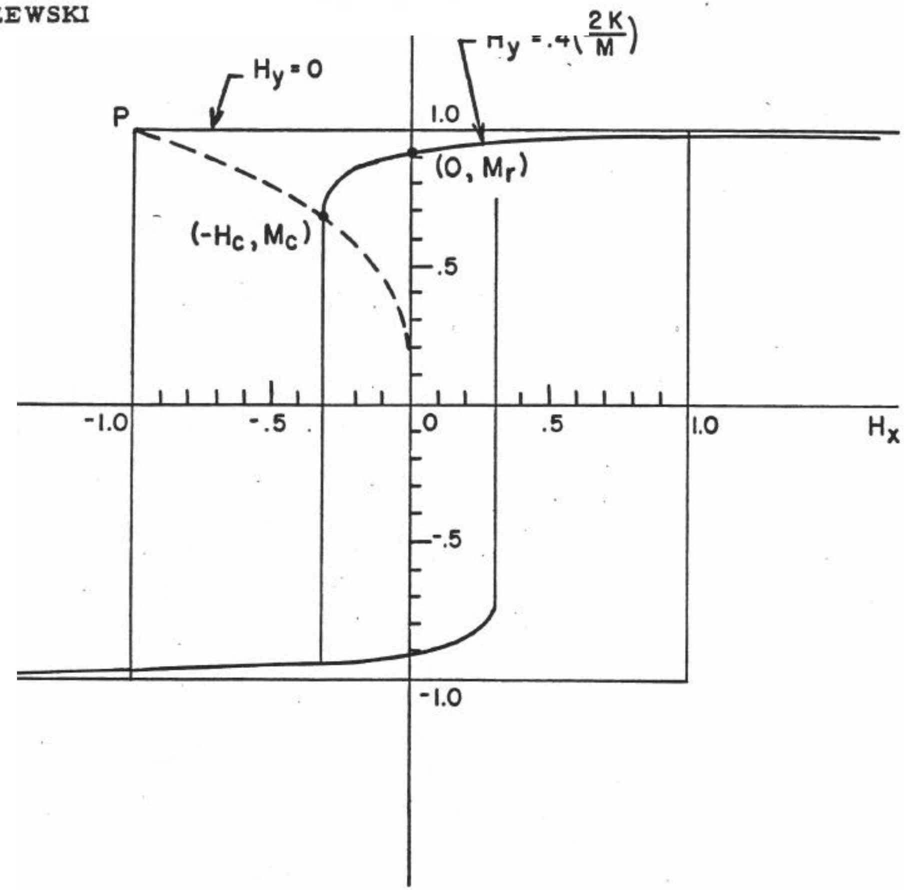

STATIC CRITICAL CURVE

The free energy of a uniaxial anisotropy single domain particle

$$W(\theta,\mathbf{H}) = K_1 \sin^2\theta - \mathbf{M}.\mathbf{H} \longrightarrow \frac{\partial W}{\partial \theta} = 0; \quad \frac{\partial^2 W}{\partial \theta^2} = 0 \longrightarrow h_x = \sin^3\theta; \quad h_y = -\cos^3\theta$$

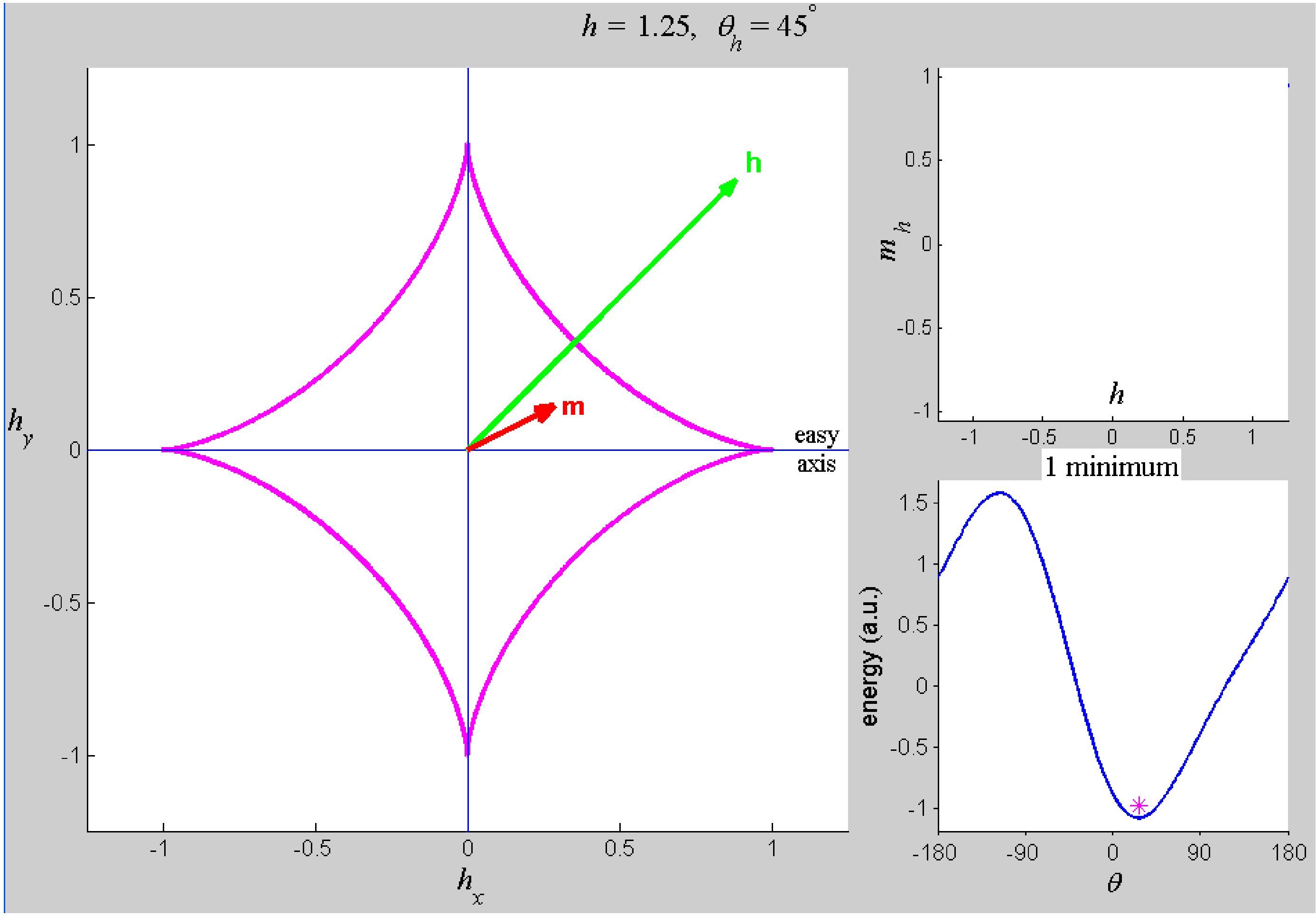

CC = the locus of in-plane fields at which the irreversible magnetization reversal occurs

J. C. Slonczewski, IBM Research Center Memorandum R. M. Report No. 003.111.224.

Classical and quantum magnetization reversal studied in nanometer-sized particles and clusters

Edited by

to be published in: Advances in Chemical Physics
invitation from Stuart A. Rice
Second version of 31 Dec. 2000

Author

Wolfgang Wernsdorfer
Lab. L. Néel - CNRS, BP166,
38042 Grenoble Cedex 9, France,
e-mail : wernsdor@labs.polycnrs-

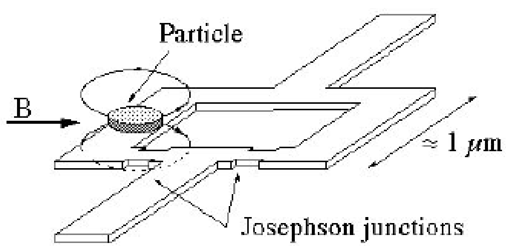

Fig. 1.5 Schematic drawing of a planar micro-bridge-DC-SQUID on which a ferromagnetic particle is placed. The SQUID detects the flux through its loop produced by the sample magnetization. Due to the close proximity between sample and SQUID a very efficient and direct flux coupling is achieved.

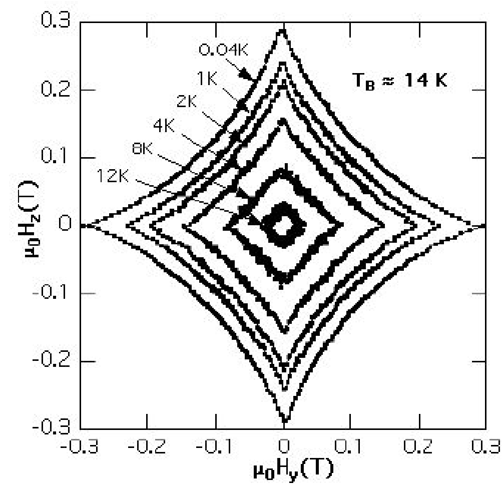

Fig. 3.3 Temperature dependence of the switching field of a 3 nm Co cluster, measured in the plane defined by the easy and medium hard axes ($H_y - H_z$ plane in Fig. 2.6). The data were recorded using the blind mode method (Sect. 1.2.6) with a waiting time of the applied field of $\Delta t = 0.1$s. The scattering of the data is due to stochastic and in good agreement with Eq. 3.10.

CRITICAL CURVE: Experiments

APPLIED PHYSICS LETTERS VOLUME 76, NUMBER 5 31 JANUARY 2000

Two-dimensional magnetic switching of micron-size films in magnetic tunnel junctions

A. Anguelouch, B. D. Schrag, and Gang Xiao
Department of Physics, Brown University, Providence, Rhode Island 02912

Yu Lu, P. L. Trouilloud, R. A. Wanner, and W. J. Gallagher
IBM T. J. Watson Research Center, Yorktown Heights, New York 1

S. S. P. Parkin
IBM Almaden Research Center, San Jose, California 95120

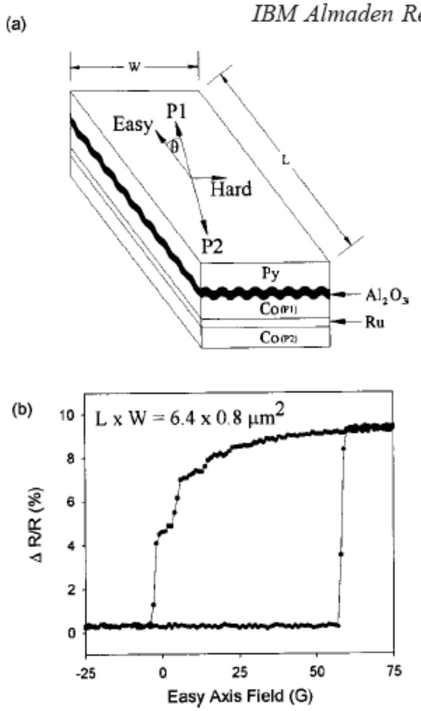

FIG. 1. (a) Schematic of the sample layer structure. The two cobalt layers will align antiparallel due to interlayer exchange across the thin Ru layer. Néel coupling occurs as a result of interface roughness at the tunneling barrier, as shown. The pinned axis (represented by P1 and P2) is assumed to be slightly misaligned with respect to the easy axis of the sample. (b) Mangetoresistance hysteresis loop, with zero applied hard-axis field.

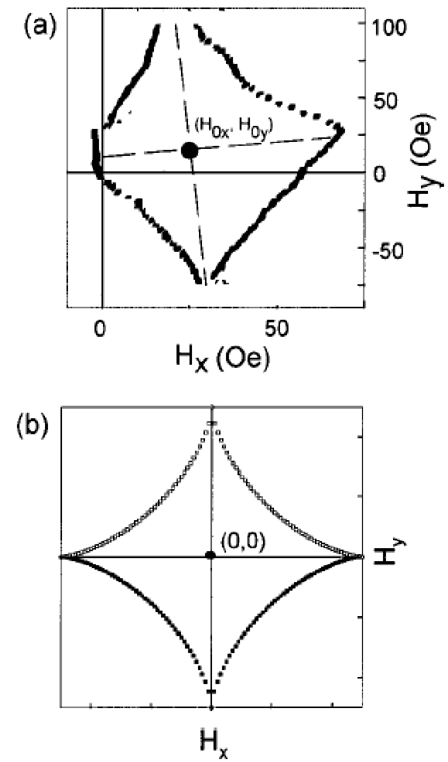

FIG. 2. (a) Asteroid curve of one representative MTJ with dimensions 0.8 $\times$6.4 μm^2. H_x and H_y are fields in the easy- and hard-axis directions. (b) Stoner–Wohlfarth critical curve for an ideal single-domain particle with uniaxial anisotropy.

Static Critical Curve: Hypocycloid

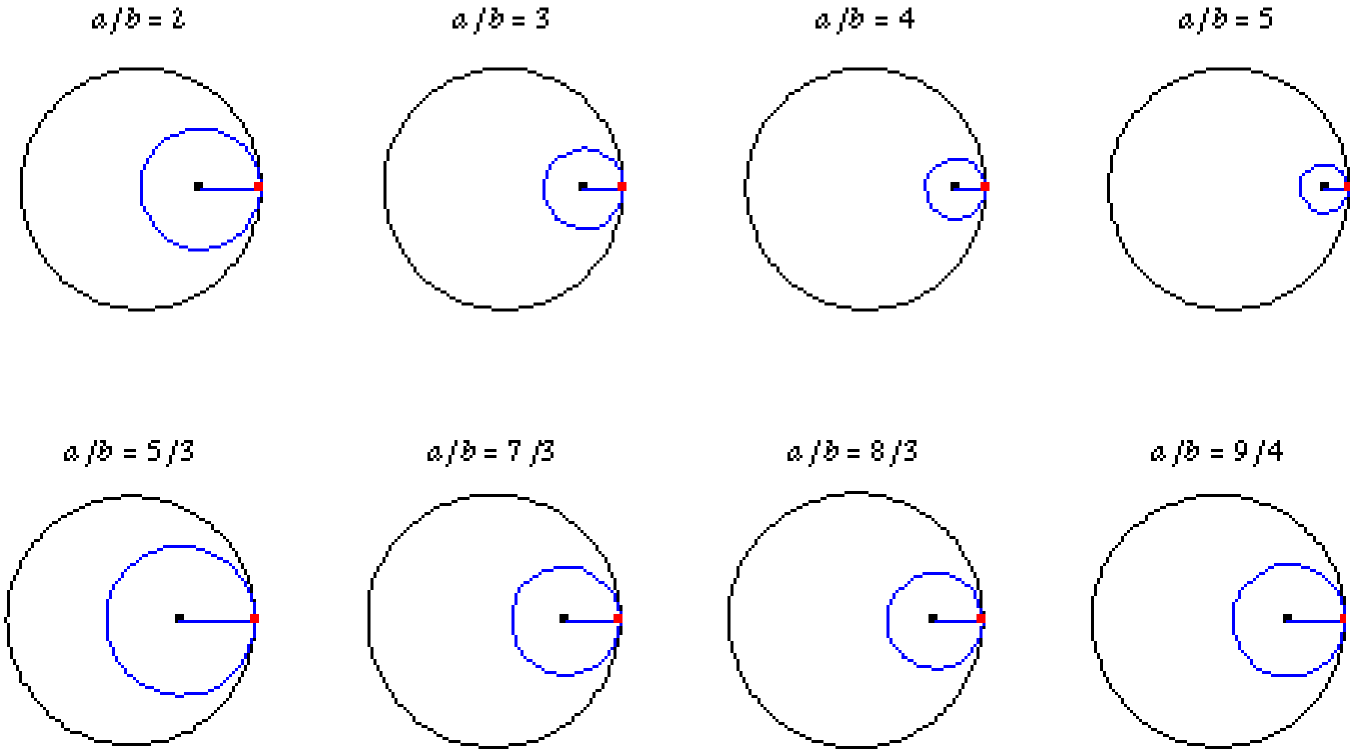

STONER-WOHLFARTH & CRITICAL CURVE

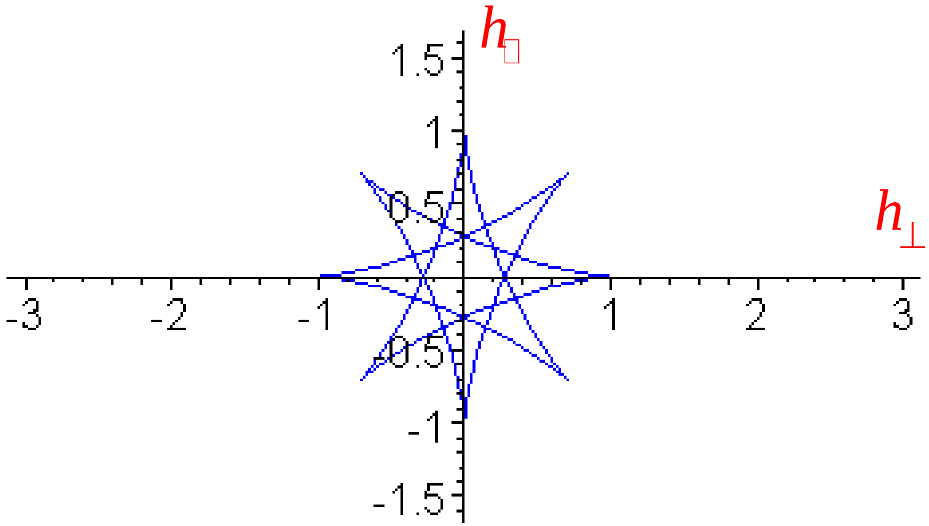

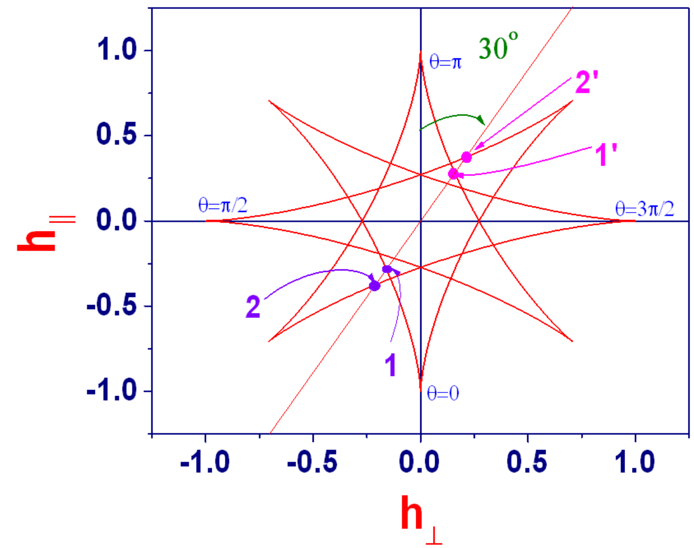

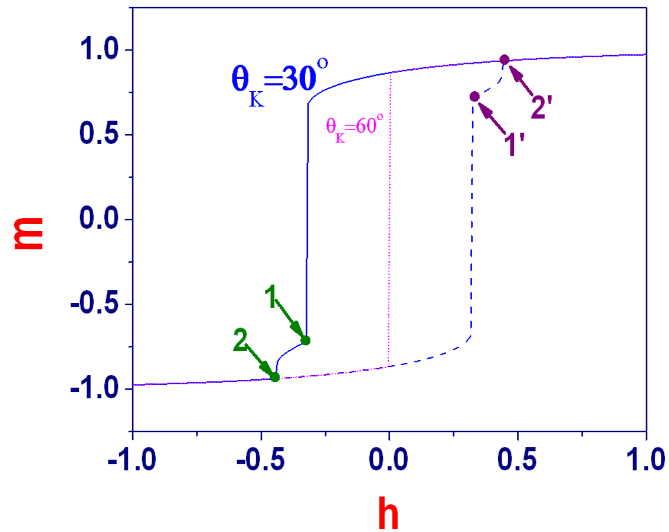

K_1, and K_2

Micromagnetic studies of coherent rotation with quartic crystalline anisotropy

Ching-Ray Chang

Department of Physics, National Taiwan University, Taipei, Taiwan, Republic of China

(Received 28 August 1990; accepted for publication 23 October 1990)

CRITICAL CURVE: Experiments

Critical curves for determining magnetization directions in implanted garnet films

C. C. Shir[a)] and Y. S. Lin

IBM Thomas J. Watson Research Center, Yorktown Heights, New York 10598

(Received 28 September 1978; accepted for publication 15 December 1978)

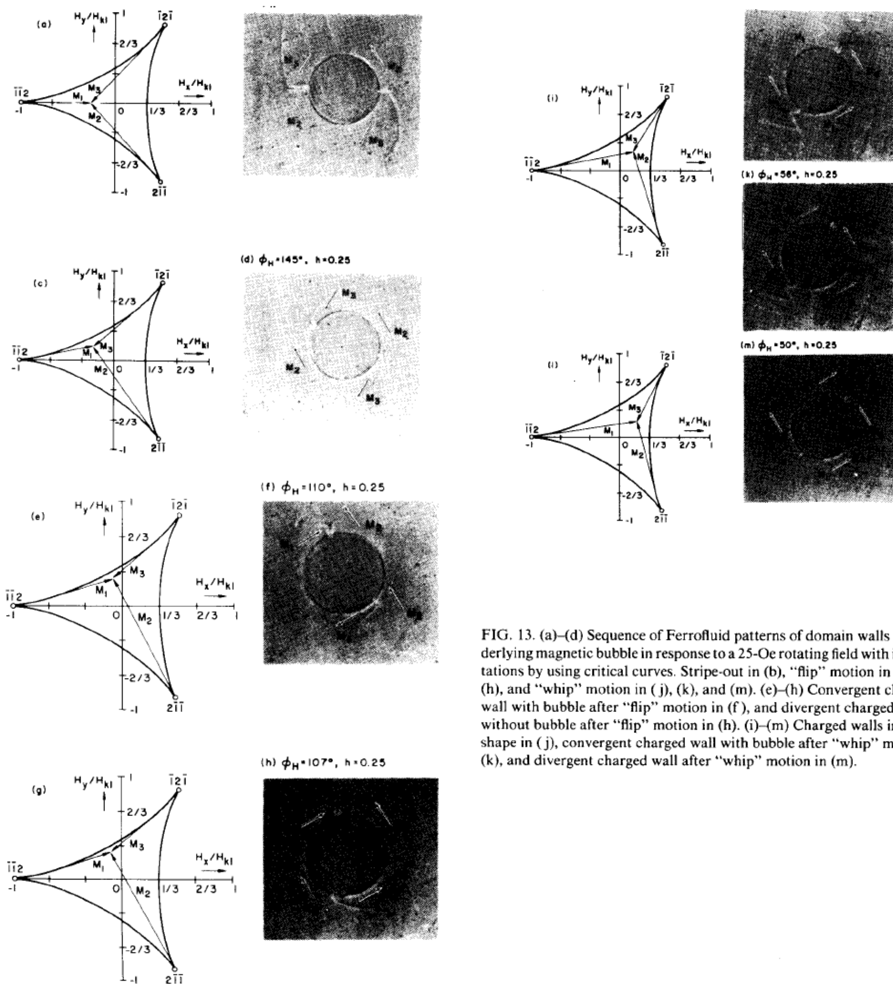

FIG. 13. (a)–(d) Sequence of Ferrofluid patterns of domain walls and underlying magnetic bubble in response to a 25-Oe rotating field with interpretations by using critical curves. Stripe-out in (b), "flip" motion in (d), (f), (h), and "whip" motion in (j), (k), and (m). (e)–(h) Convergent charged wall with bubble after "flip" motion in (f), and divergent charged wall without bubble after "flip" motion in (h). (i)–(m) Charged walls in zigzag shape in (j), convergent charged wall with bubble after "whip" motion in (k), and divergent charged wall after "whip" motion in (m).

Experimental CC: Susceptibility Method

- **Introducing our new sensitive method based on reversible susceptibility's singularities detection for determination of the critical curve of 2D magnetic systems**

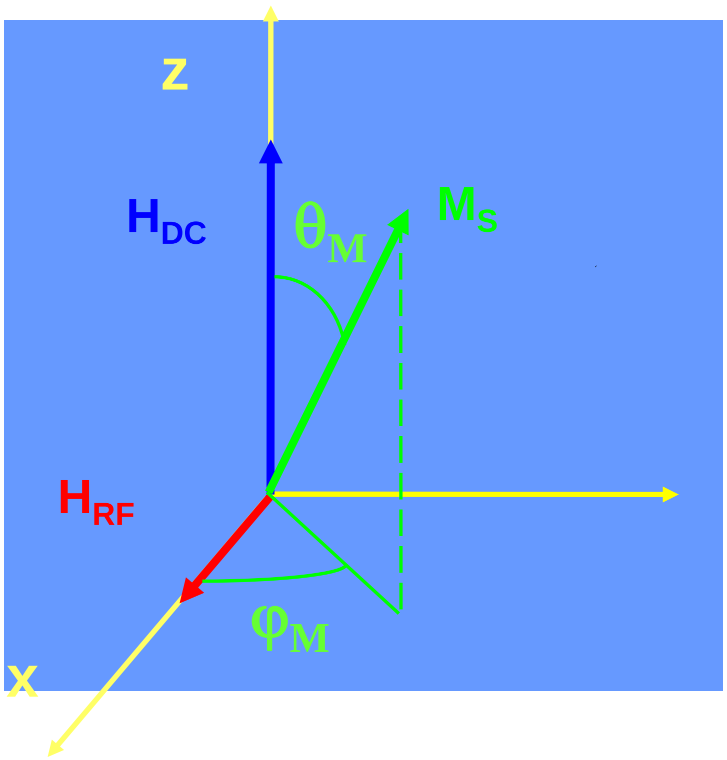

$$\chi_{ij} = \lim_{\Delta H_j \to 0} \frac{\Delta M_i}{\Delta H_j}$$

$$\chi_T = \chi_{xx} = \left(\frac{dM_x}{dH_x} \right)_{H_z = H_y = 0}$$

Experimental CC: Susceptibility Method

Available online at www.sciencedirect.com

SCIENCE DIRECT®

ELSEVIER

Journal of Magnetism and Magnetic Materials 296 (2006) 1–8

journal of magnetism and magnetic materials

www.elsevier.com/locate/jmmm

Letter to the Editor

Transverse susceptibility as the low-frequency limit of ferromagnetic resonance

L. Spinu[a,*], I. Dumitru[b], A. Stancu[c], D. Cimpoesu[c]

[a]*Advanced Materials Research Institute and Department of Physics, University of New Orleans, 2000 Lakeshore Drive, New Orleans, LA 70148, USA*
[b]*Advanced Materials Research Institute, University of New Orleans, New Orleans, LA 70148, USA*
[c]*Faculty of Physics, "Al.I. Cuza" University, Iasi 700506, Romania*

Received 2 December 2004; received in revised form 6 December 2004
Available online 7 March 2005

The TS tensor components

$$\chi_{xx} = \frac{M^2}{F_{\theta\theta}F_{\varphi\varphi} - F_{\theta\varphi}^2}\left(\sin^2\theta_M \sin^2\varphi_M F_{\theta\theta} + \frac{\sin 2\theta_M \sin 2\varphi_M}{2} F_{\theta\varphi} + \cos^2\theta_M \cos^2\varphi_M F_{\varphi\varphi}\right)$$

$$\chi_{yy} = \frac{M^2}{F_{\theta\theta}F_{\varphi\varphi} - F_{\theta\varphi}^2}\left(\sin^2\theta_M \cos^2\varphi_M F_{\theta\theta} - \frac{\sin 2\theta_M \sin 2\varphi_M}{2} F_{\theta\varphi} + \cos^2\theta_M \sin^2\varphi_M F_{\varphi\varphi}\right)$$

$$\chi_{zz} = \frac{M^2}{F_{\theta\theta}F_{\varphi\varphi} - F_{\theta\varphi}^2}\left(\sin^2\theta_M F_{\varphi\varphi}\right)$$

Probing 2D switching using susceptibility experiments

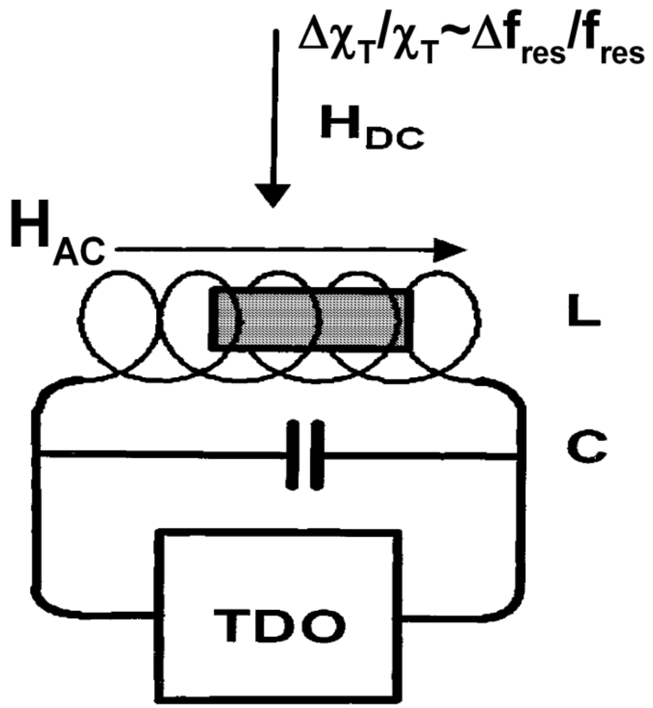

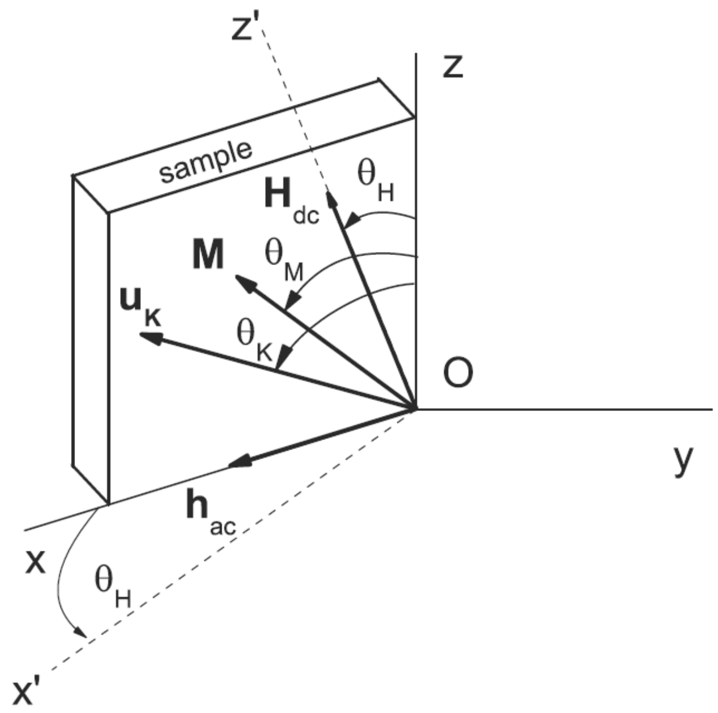

$$D\left(\theta_M, \varphi_M\right) = F_{\theta\theta} F_{\varphi\varphi} - F_{\theta\varphi}^2, \qquad \chi_{xx} \propto 1/D\left(\theta_M, \varphi_M\right).$$

The theoretical curve

The experimental curve

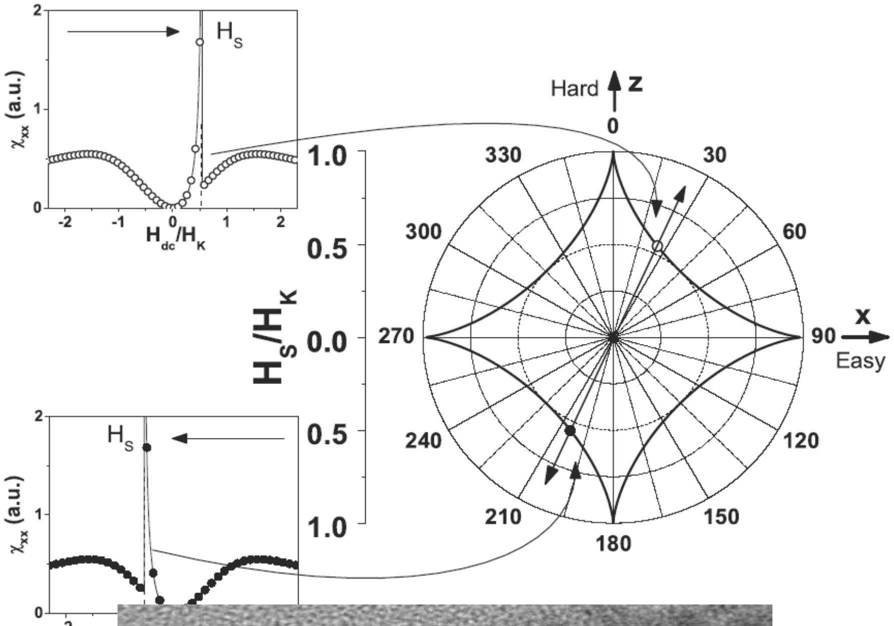

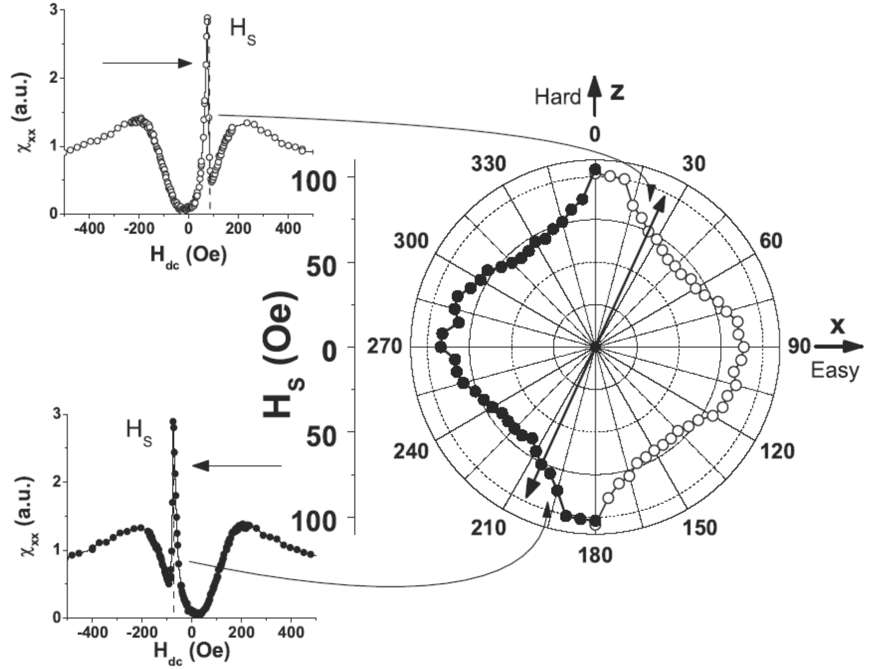

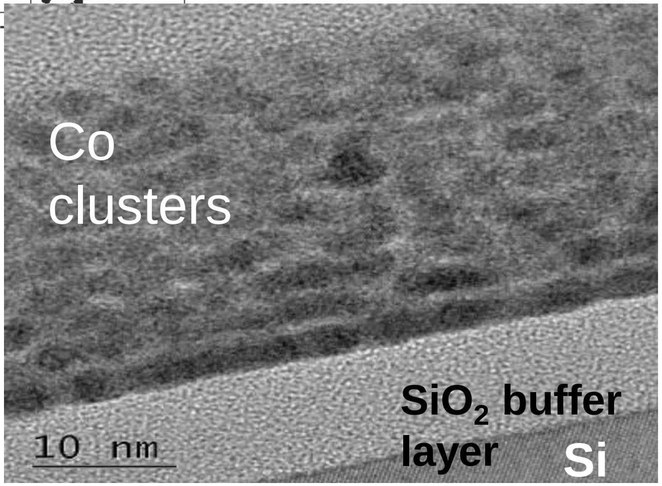

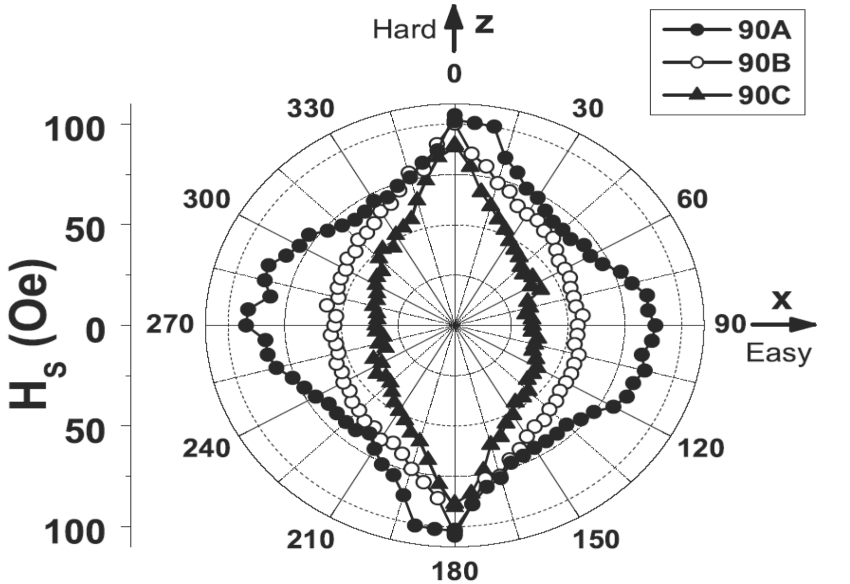

APPLIED PHYSICS LETTERS **86**, 012506 (2005)

Probing two-dimensional magnetic switching in Co/SiO_2 multilayers using reversible susceptibility experiments

L. Spinu,[a] H. Pham, and C. Radu
Advanced Materials Research Institute and Department of Physics, University of New Orleans, New Orleans, Louisiana 70148

RAPID COMMUNICATIONS

PHYSICAL REVIEW B **68**, 220401(R) (2003)

Vectorial mapping of exchange anisotropy in IrMn/FeCo multilayers using the reversible susceptibility tensor

L. Spinu*
Advanced Materials Research Institute and Department of Physics, University of New Orleans, New Orleans, Louisiana 70148, USA

Al. Stancu
Faculty of Physics, "Al.I. Cuza" University, Iasi 6600, Romania

Y. Kubota, G. Ju, and D. Weller
Seagate Research, Pittsburgh, Pennsylvania 15222, USA

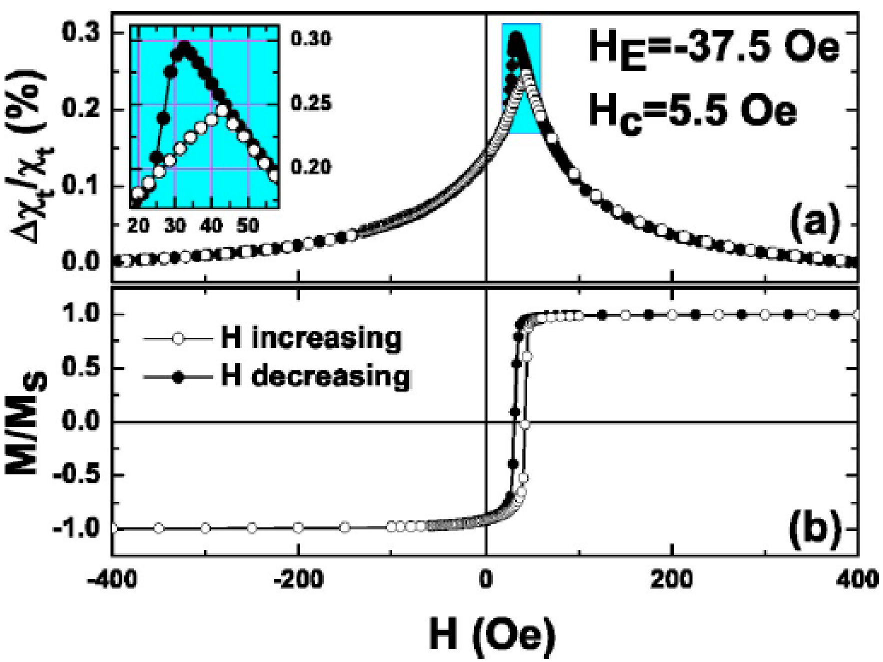

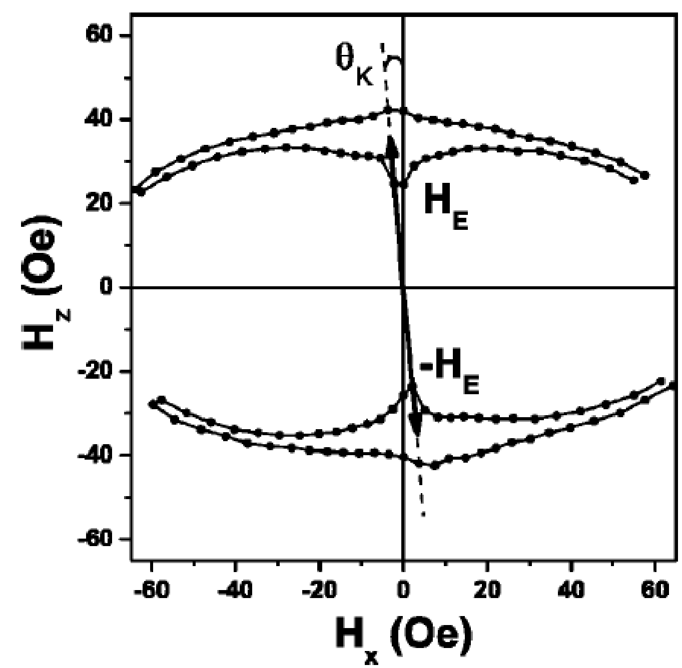

Static vs. Dynamic

LETTERS

Switching of magnetization by nonlinear resonance studied in single nanoparticles

CHRISTOPHE THIRION[1], WOLFGANG WERNSDORFER*[1] DOMINIQUE MAILLY[2]
[1]Laboratoire Louis Néel, associé à l'UJF, CNRS, BP 166, 38042 Grenoble Cedex 9, France
[2]Laboratoire de photonique et de nanostructures, CNRS, Route de Nozay, 91460 Marcoussis, France
*e-mail: wernsdor@grenoble.cnrs.fr

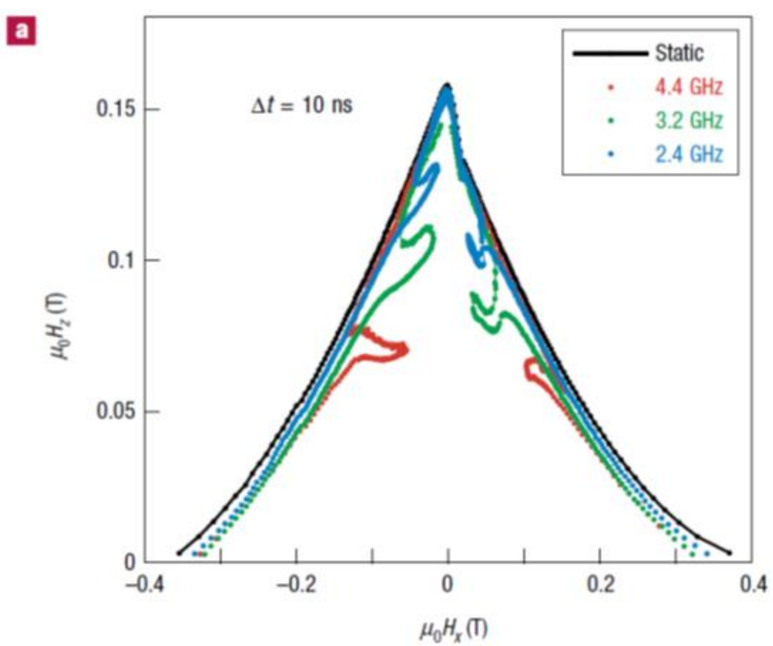

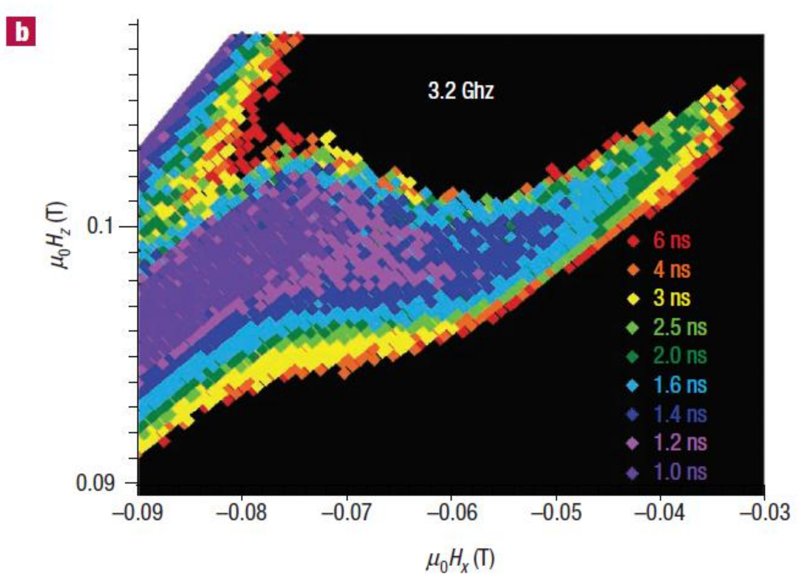

DYNAMIC MAGNETIZATION SWITCHING

Ellipsoidal permalloy Particle

$4\pi M_S = 10.8$ kG

$N_x = 0.008$

$N_y = 0.012$

$N_z = 0.980$

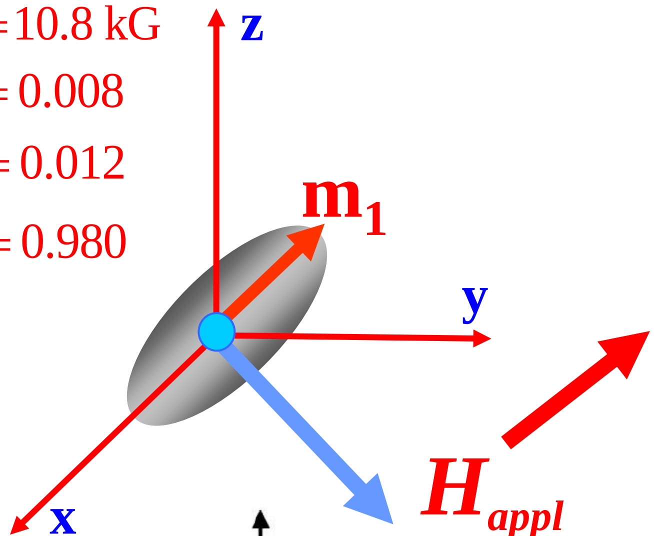

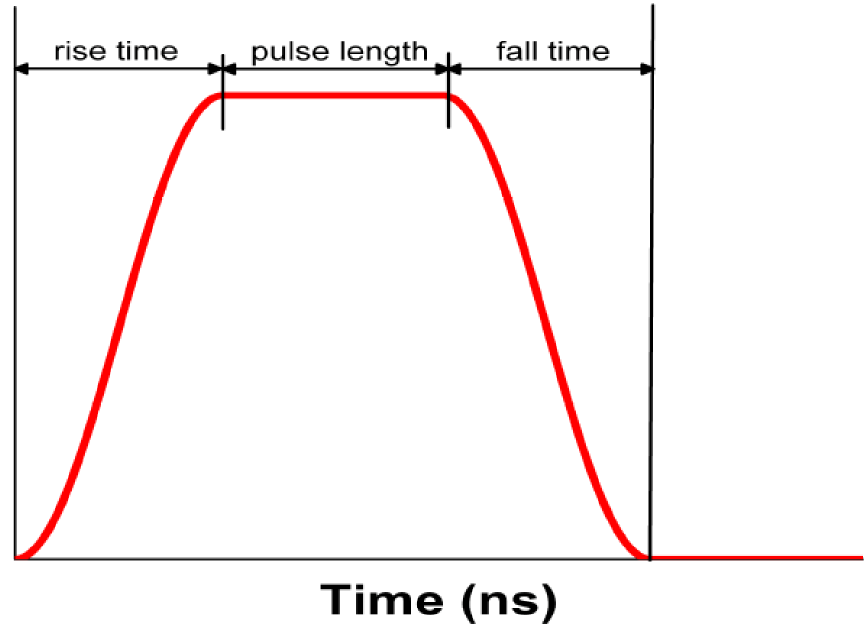

pulse:
0.0/2.75/0.0

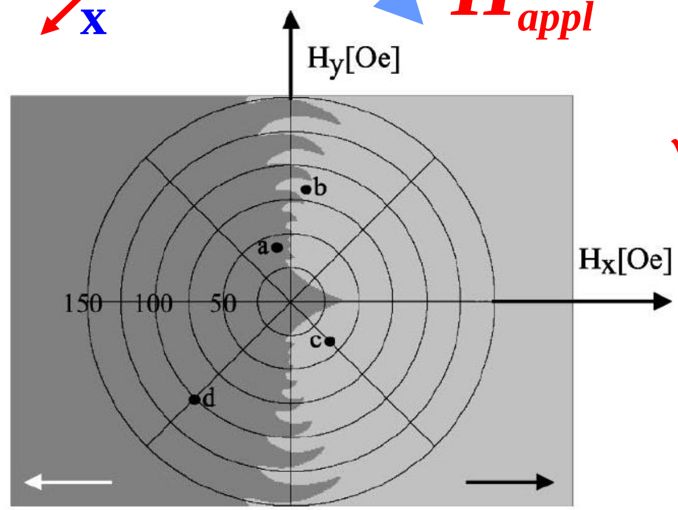

✓**Scheme of the pulse to explain the parameters**

pulse rise time/pulse length/pulse fall time

PHYSICAL REVIEW B VOLUME 61, NUMBER 5 1 FEBRUARY 2000-I

Switching behavior of a Stoner particle beyond the relaxation time limit

M. Bauer, J. Fassbender,* and B. Hillebrands

MAGNETIZATION SWITCHING DIAGRAM

Applied Pulse **0/0.25/0 ns**

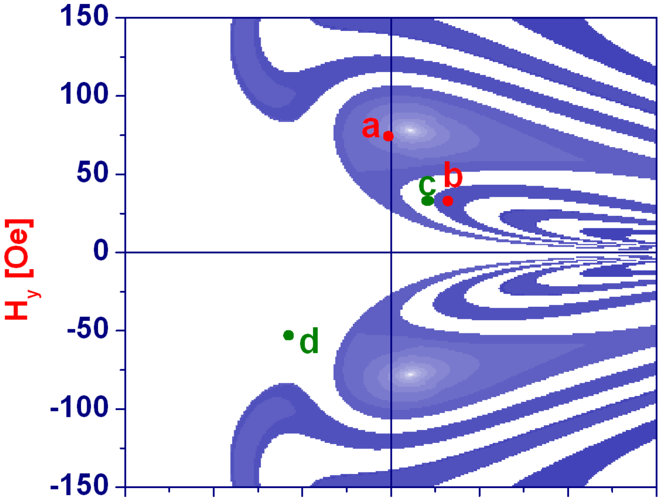

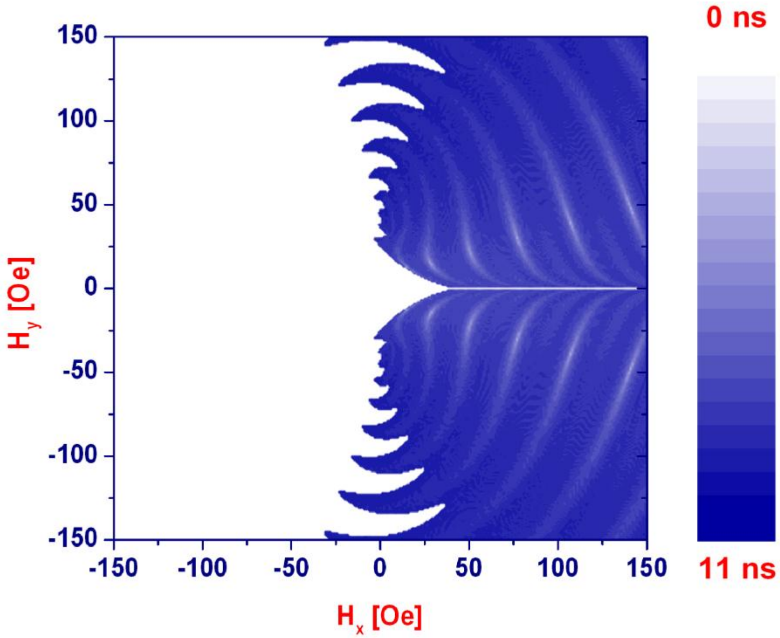

Applied Pulse **0/2.75/0 ns**

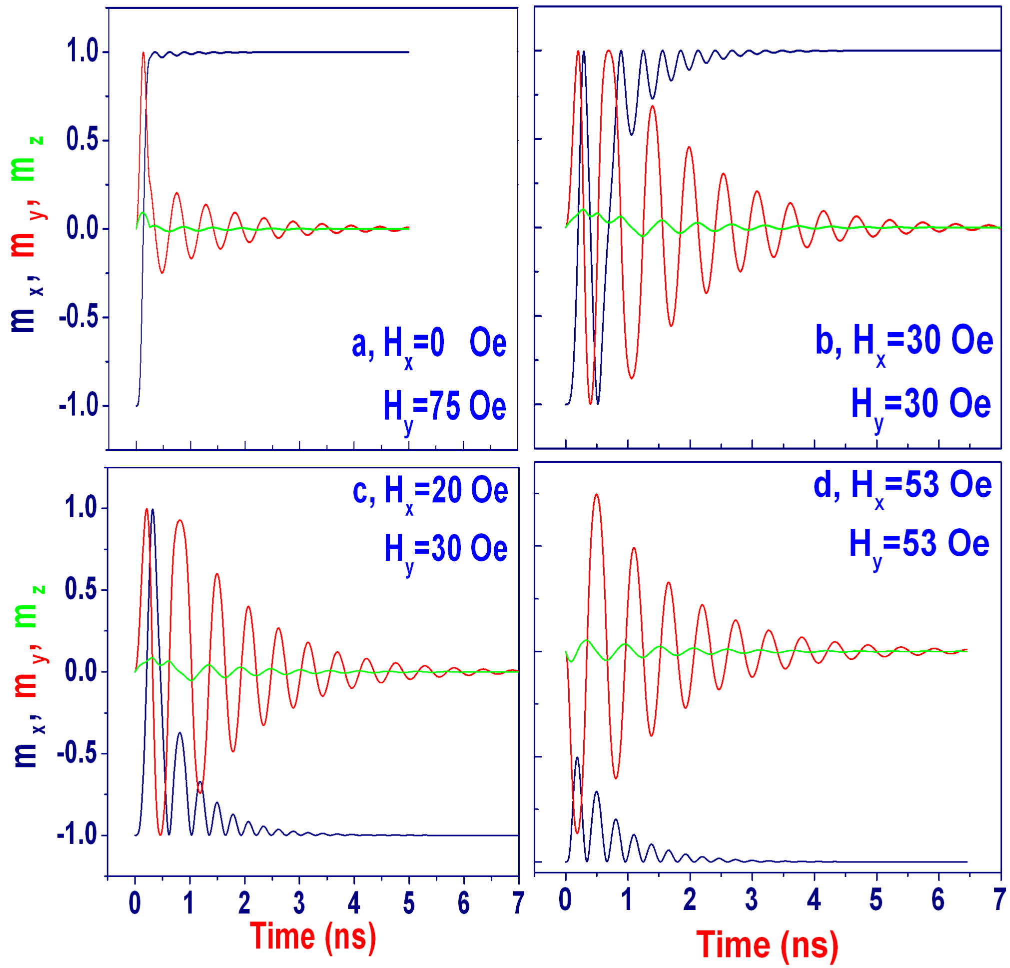

Static Critical Curve .vs. Dynamic Critical Curve

DC Applied Field

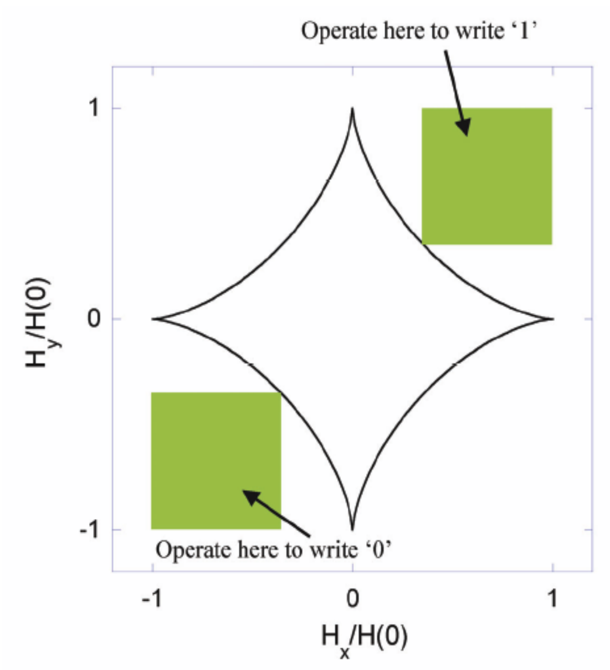

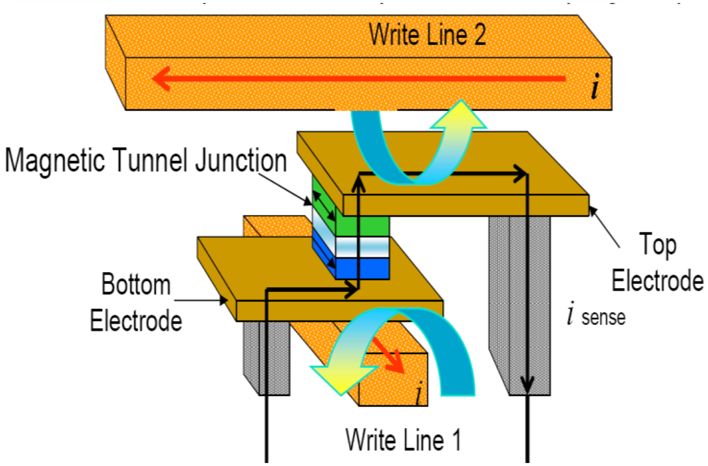

Applied Pulse 0/2.75/0 ns

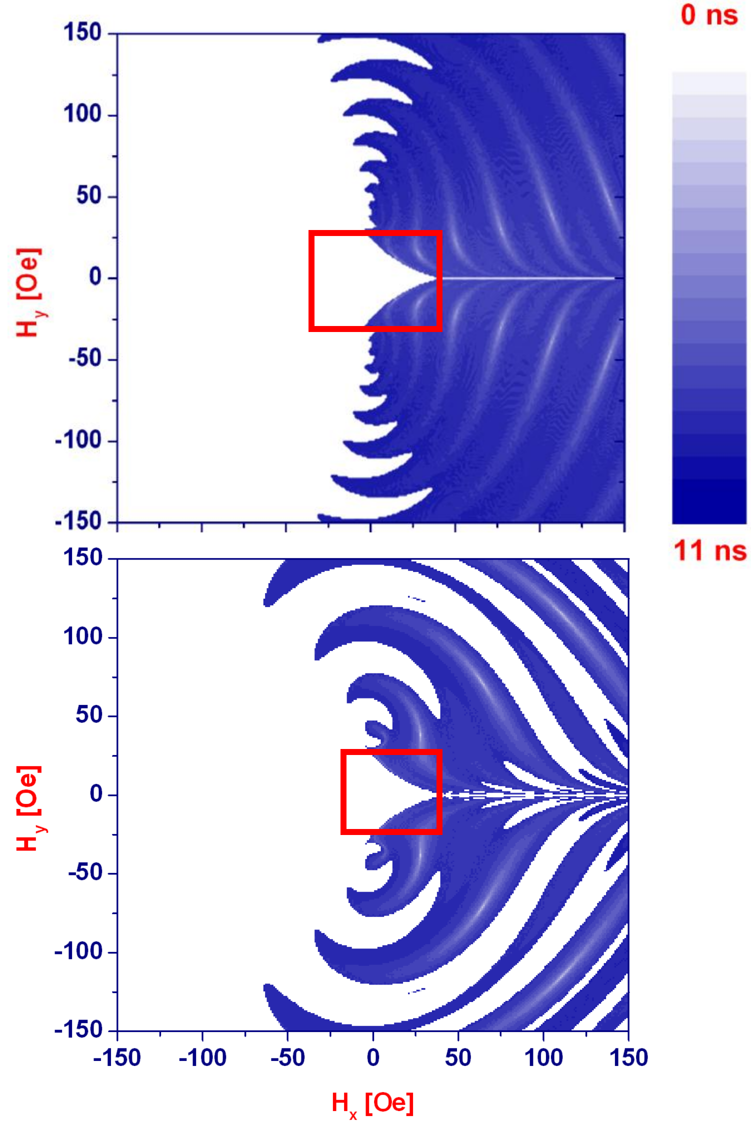

Applied Pulse 0/1.4/0 ns

The Nobel Prize in Physics 2007

Discovery of Giant Magnetoresistence

Albert Fert

Peter Grunberg

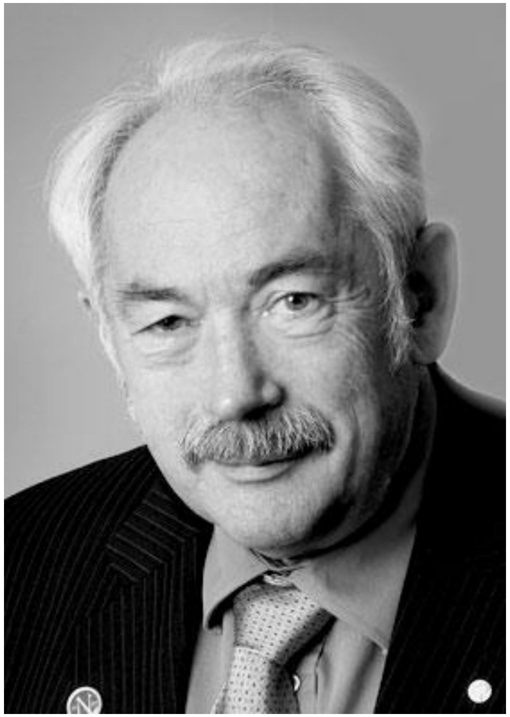

MTJ FOR MRAM EVOLUTION

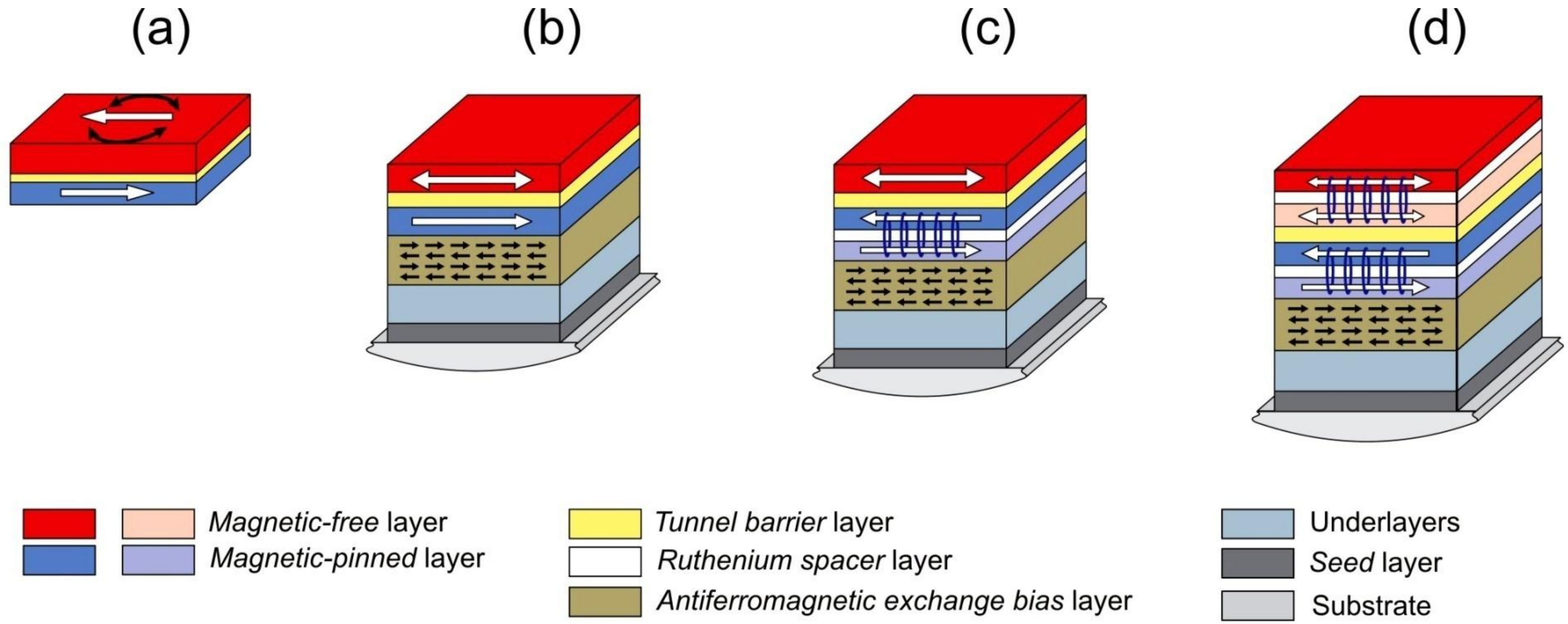

(a) basic magnetic tunnel junction structure consisting of two ferromagnetic metals separated by a thin insulating layer

(b) exchange-coupling one of the magnetic layers to an antiferromagnetic layer (by "pinning" the layer) the TMR response reflects the hysteresis of the other so-called "free" layer and has a response more suitable for memory

(c) magnetic offset caused by fields emanating from the pinned layer -> SAF pinned layer; the lower layer in this artificial antiferromagnet is pinned via exchange bias. This flux closure increases the magnetic stability of the pinned layer and reduces coupling to the free layer

(d) both pinned and free = antiferromagnetically coupled pairs -> used in toggle-MRAM

Synthetic antiferromagnet (SAF) structures

- The synthetic antiferromagnet **(SAF)** = a nanostructured sandwich of two ferromagnetic thin films antiferromagnetically coupled through a non-magnetic metallic spacer.

- Many technological applications:
  - soft underlayer for perpendicular recording
  - hard disk reading heads
  - magnetic sensors
  - **MRAM**
  - **Toggle-MRAM**

SAF

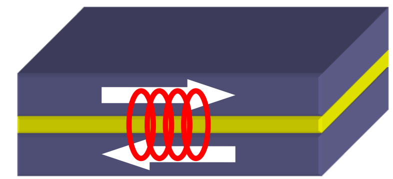

MRAM

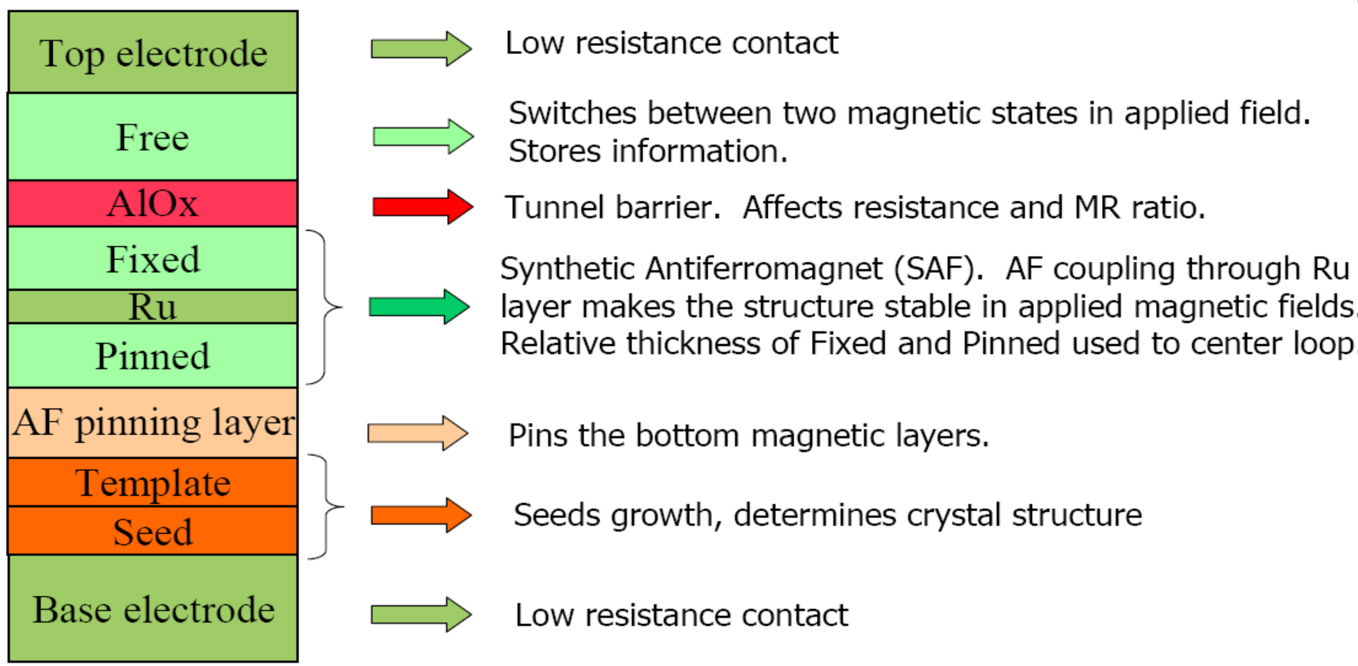

Comparison between the Non-Coupled and Coupled Magnetic Structures

	Non-Coupled	Coupled
Magnetization vectors	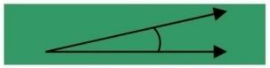 $\mathrm{M} = M \measuredangle \theta$	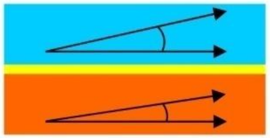 $\mathrm{M}_1 = M_1 \measuredangle \theta_1$ $\mathrm{M}_2 = M_2 \measuredangle \theta_2$
Major easy axes	$\theta = 0$	$\theta_1 = 0 \;,\; \theta_2 = \alpha$
Total free energy	**Anisotropy energy +** **+ magnetization energy**	**Anisotropy energy 1 +** **Anisotropy energy 2 +** **+ magnetization energy 1 (due to applied field) +** **+ magnetization energy 2 (due to applied field) +** **+ magnetization energy (due to interacting field)**
Stable states (corresponding to minimum energy) are determined by solving equations shown	$\partial F / \partial \theta = 0$, **subject to the condition** $\dfrac{\partial^2 F}{\partial \theta^2} > 0$	$\partial F / \partial \theta_1 = \partial F / \partial \theta_2 = 0$, **subject to the conditions** $\dfrac{\partial^2 F}{\partial \theta_1^2} > 0$ and $\left(\dfrac{\partial^2 F}{\partial \theta_1 \partial \theta_2}\right)^2 - \dfrac{\partial^2 F}{\partial \theta_1^2}\dfrac{\partial^2 F}{\partial \theta_2^2} < 0$
Critical states	**Limiting case of stable states** $\partial F / \partial \theta = 0$ $\partial^2 F / \partial \theta^2 = 0$	**Limiting case of stable states** $\partial F / \partial \theta_1 = \partial F / \partial \theta_2 = 0$ $\partial^2 F / \partial \theta_1^2 = 0$ or $\partial^2 F / \partial \theta_2^2 = 0$ or $\left(\dfrac{\partial^2 F}{\partial \theta_1 \partial \theta_2}\right)^2 - \dfrac{\partial^2 F}{\partial \theta_1^2}\dfrac{\partial^2 F}{\partial \theta_2^2} = 0$
Convenient description	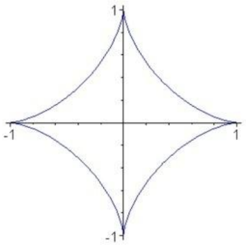	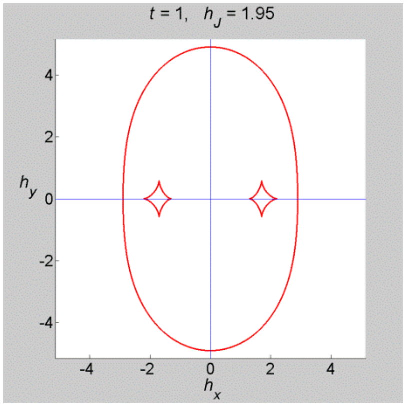

Hsu Chang

Analysis of Static and Quasidynamic Behavior of Magnetostatically Coupled Thin Magnetic Films

Abstract: When two superposed films exert fields on each other, their static and dynamic behaviors change. The following method of analysis is used to study the behavior: The stable states are found by minimizing the total free energy of the films. Then constant-field contours are plotted in the θ_1-θ_2 plane (θ's being the stable orientations of the magnetization vectors). In examining the plot, one can predict multiple stable states, switching, threshold, hysteresis, and the detailed paths of magnetization change as a function of applied field.

The solution is carried out by a numerical process which permits evaluation of the following effects: the variation of the degrees of symmetries of the anisotropy energies, the relative orientation between the films, the coupling strength, and the drive-line layout. An example is carried out in sufficient detail for illustrative purposes.

H. Chang, "Analysis of static and quasidynamic behavior of magneostatically coupled thin magnetic films," IBM J. Res. Dev., vol. 6, pp. 419-429, 1962.

Table 2 **Comparison between single film and pair of magnetostatically coupled films.**

	Single film	*Coupled films*
Magnetization vectors	$\mathbf{M} = M\angle\theta$	$\mathbf{M}_1 = M_1\angle\theta_1; \mathbf{M}_2 = M_2\angle\theta_2$
Major easy axes	$\theta = 0$	$\theta_1 = 0, \theta_2 = \alpha$
Total free energy	Anisotropy energy + magnetization energy	Anisotropy energies + magnetization energies (due to applied field) + magnetization energy (due to interacting field)
Stable states (corresponding to minimum energy) are determined by solving equations shown	$\partial E/\partial\theta = 0$, subject to the condition $\dfrac{\partial^2 E}{\partial\theta^2} > 0$	$\partial E/\partial\theta_1 = \partial E/\partial\theta_2 = 0$ subject to the conditions $\dfrac{\partial^2 E}{\partial\theta_1^2} > 0$ and $\left(\dfrac{\partial^2 E}{\partial\theta_1\partial\theta_2}\right)^2 - \dfrac{\partial^2 E}{\partial\theta_1^2}\dfrac{\partial^2 E}{\partial\theta_2^2} < 0$
Critical states	Limiting case of stable states $\partial E/\partial\theta = 0$ $\partial^2 E/\partial\theta^2 = 0$	Limiting case of stable states $\partial E/\partial\theta_1 = \partial E/\partial\theta_2 = 0$ $\partial^2 E/\partial\theta_1^2 = 0$ or $\partial^2 E/\partial\theta_2^2 = 0$ or $\left(\dfrac{\partial^2 E}{\partial\theta_1\partial\theta_2}\right)^2 - \dfrac{\partial^2 E}{\partial\theta_1^2}\dfrac{\partial^2 E}{\partial\theta_2^2} = 0$
Convenient description	Critical curve and equilibrium line in h_x-h_y plane (see Appendix I and Fig. 8)	Constant field contours in θ_1-θ_2 plane (see Section of that title and also Fig. 4)

H. Chang, "Analysis of static and quasidynamic behavior of magneostatically coupled thin magnetic films," IBM J. Res. Dev., vol. 6, pp. 419-429, 1962.

Constant Angle Contour Maps

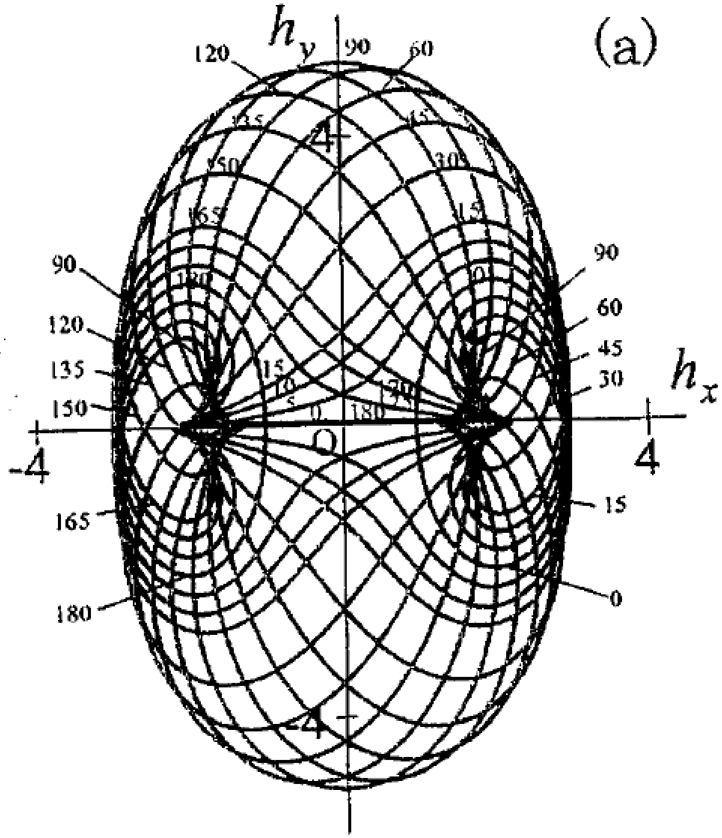

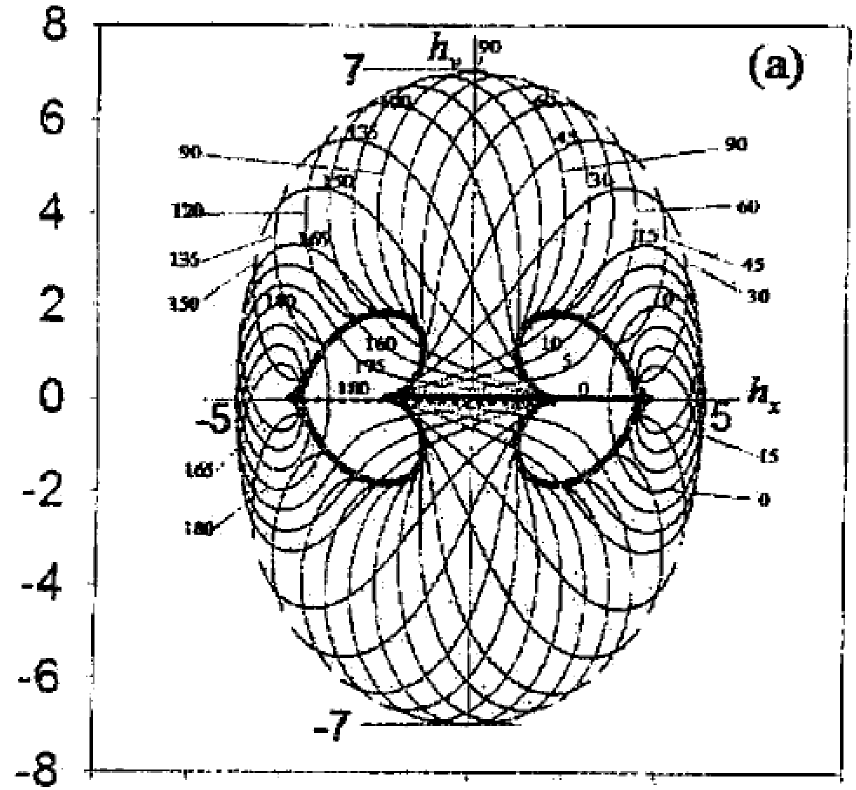

SAF CRITICAL CURVE

JOURNAL OF APPLIED PHYSICS **97**, 10P507 (2005)

Critical-field curves for switching toggle mode magnetoresistance random access memory devices (invited)

H. Fujiwara[a)] and S.-Y. Wang
Materials for Information Technology (MINT) Center and Department of Physics and Astronomy, University of Alabama, Tuscaloosa, Alabama 35487

M. Sun
Materials for Information Technology (MINT) Center and Department of Mathematics, University of Alabama, Tuscaloosa, Alabama 35487

(Presented on 9 November 2004; published online 17 May 2005)

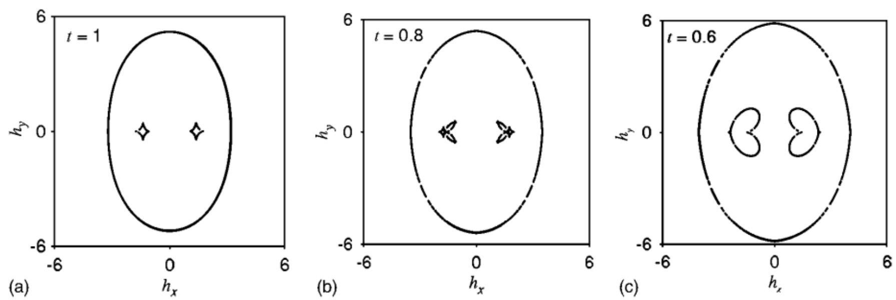

FIG. 4. Critical-field curves obtained keeping the parameters $m=1$ and $k=1$ for $t=1$, $h_{N1y}/h_{N1x}=1.5$, and $h_J=1.5$, and changing the thickness ratio t: (a) $t=1$, (b) $t=0.8$, and (c) $t=0.6$. For the same assumption as in Fig. 3 about M_s, H_{k1}, and t_1, the set of normalized parameters chosen here corresponds to the parameter set of $H_{ku1}=4$ Oe, $M_s(N_{1y}-N_{1x})=4$ Oe, and $J+rM_s^2t_2N_{1x}=0.02$ ergs/cm^2.

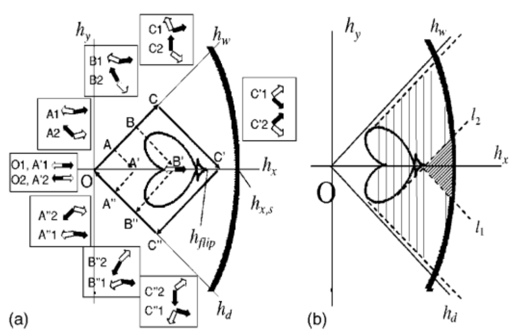

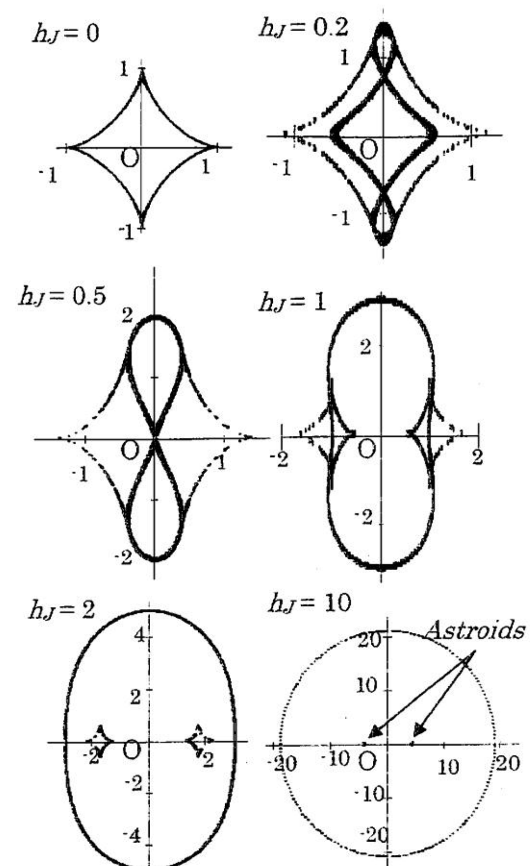

SAF Critical Curve

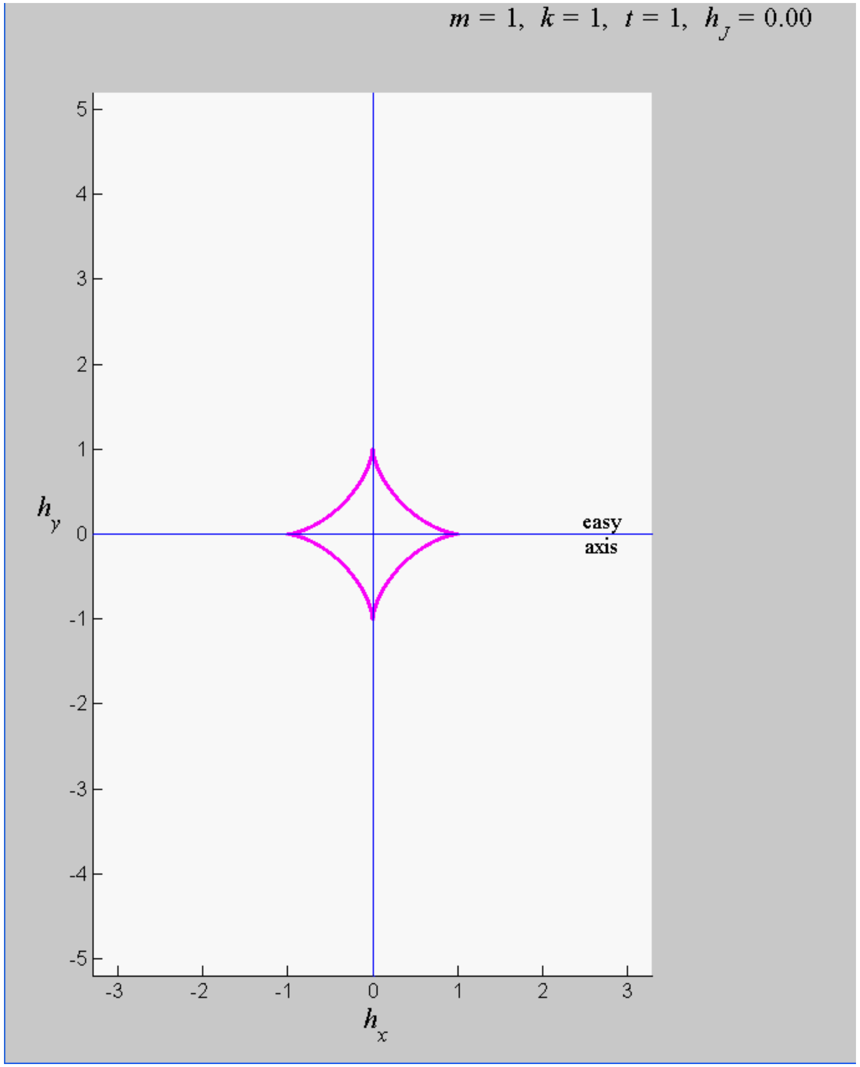

Critical Curves (CC) – Symmetric SAF

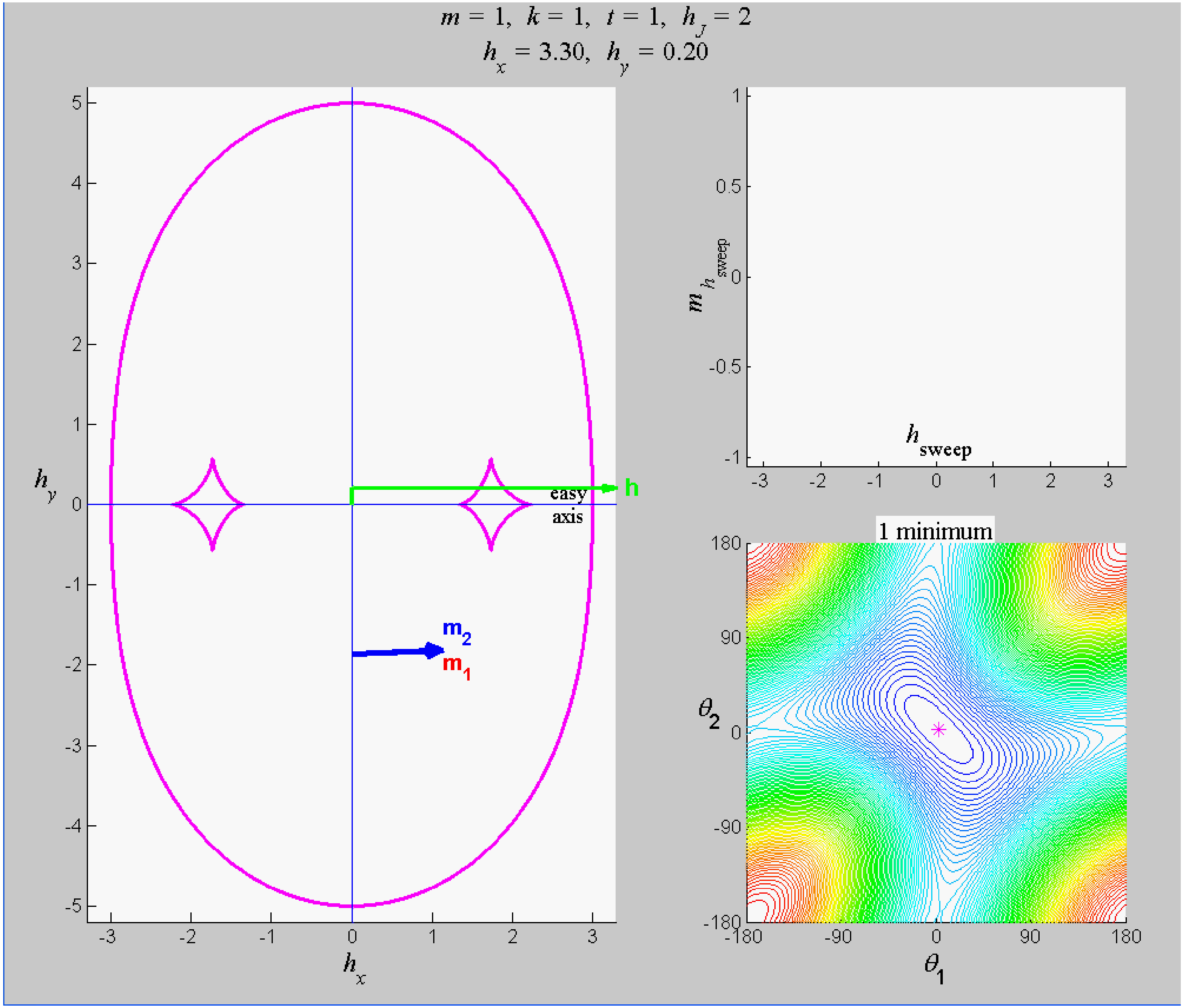

Critical Curves (CC) – Asymmetric SAF

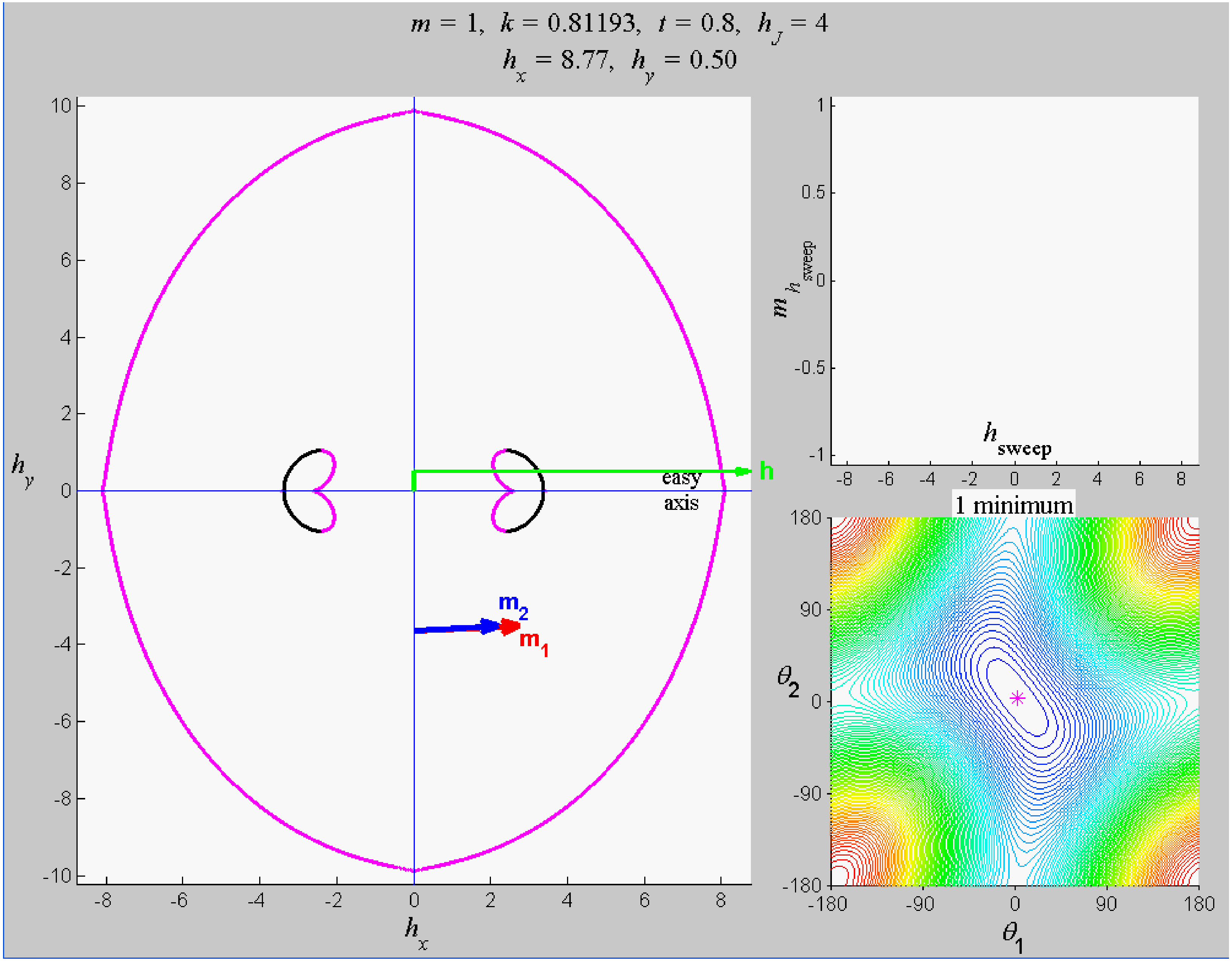

Critical Curve and Susceptibility Tensor
for a coupled structure

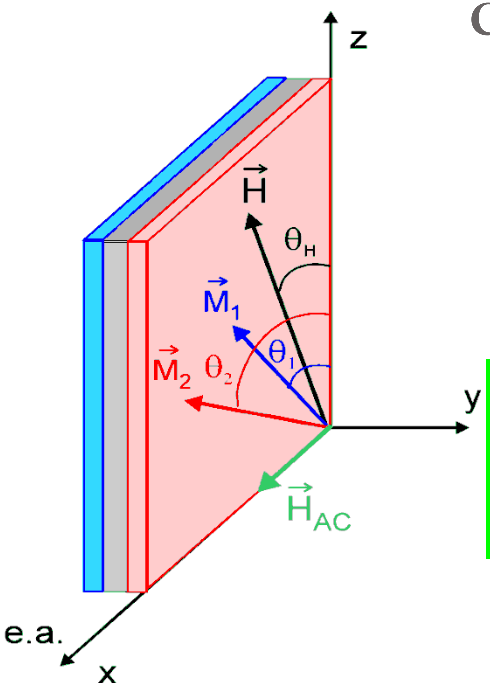

$$\frac{\partial F}{\partial \theta_1} = \frac{\partial F}{\partial \theta_2} = 0$$

$$\boxed{\left(\frac{\partial^2 F}{\partial \theta_1 \partial \theta_2}\right)^2 - \left(\frac{\partial^2 F}{\partial \theta_1^{\,2}}\right)\left(\frac{\partial^2 F}{\partial \theta_2^{\,2}}\right) = 0}$$

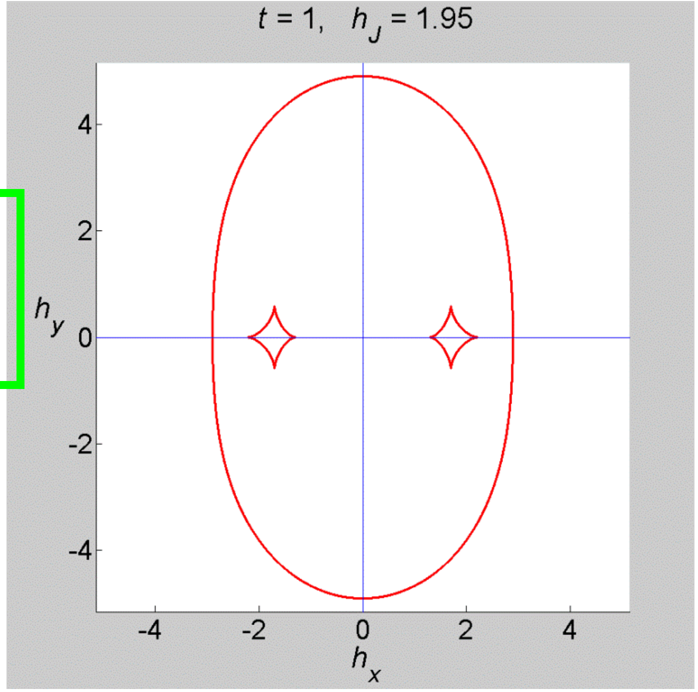

$$\chi_{xx} = \lim_{H_{ac}\to 0} \frac{\Delta M_x}{H_{ac}} = \lim_{H_{ac}\to 0} \frac{\Delta M_{1,x} + \Delta M_{2,x}}{H_{ac}}$$

F = energy density per unit area

$$= F_{\text{Zeeman}} + F_{\text{anisotropy}} + \underbrace{F_{\text{coupling}}}_{h_J\, \vec{\mathbf{m}}_1 \cdot \vec{\mathbf{m}}_2}$$

$$m = \frac{M_{2,s}}{M_{1,s}}; \quad t = \frac{t_2}{t_1}; \quad t_i = \text{thickness of layer } i$$

$$\chi_{xx} = \frac{F_{\theta_2\theta_2}\cos^2\theta_1 - 2mt\, F_{\theta_1\theta_2}\cos\theta_1\cos\theta_2 + m^2t^2\, F_{\theta_1\theta_1}\cos^2\theta_2}{\boxed{F_{\theta_1\theta_1}F_{\theta_2\theta_2} - F_{\theta_1\theta_2}^2}}$$

Measurements of the critical curve for a coupled structure

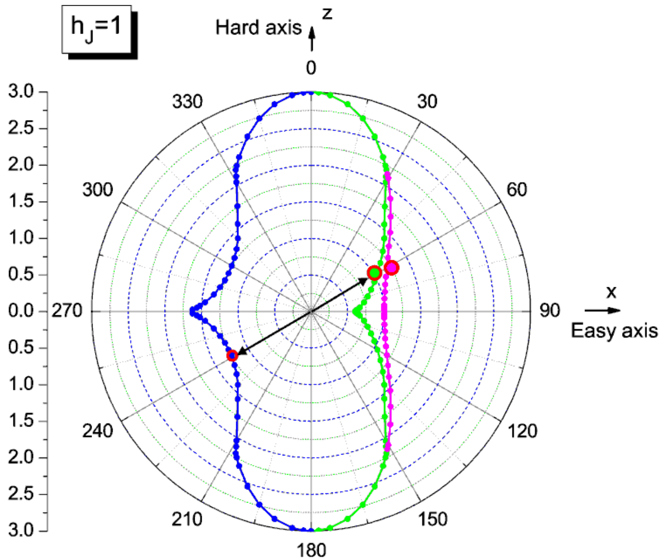

Visible advantage of using susceptibility instead of hysteresis loop

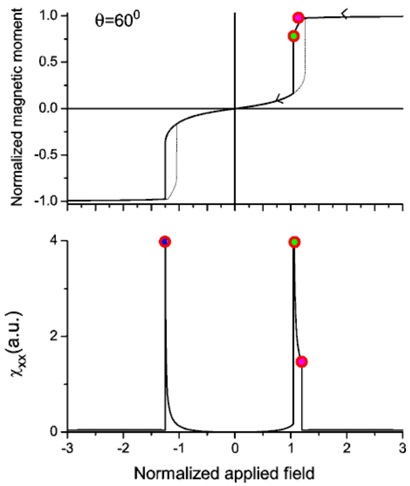

Depending on the coupling strength between the two ferromagnetic layers in a coupled (i.e. SAF) structure the critical curve evolves from a simple astroid at zero coupling to more complicated critical curves for larger coupling field values.

Measurements of the critical curve for a coupled structure

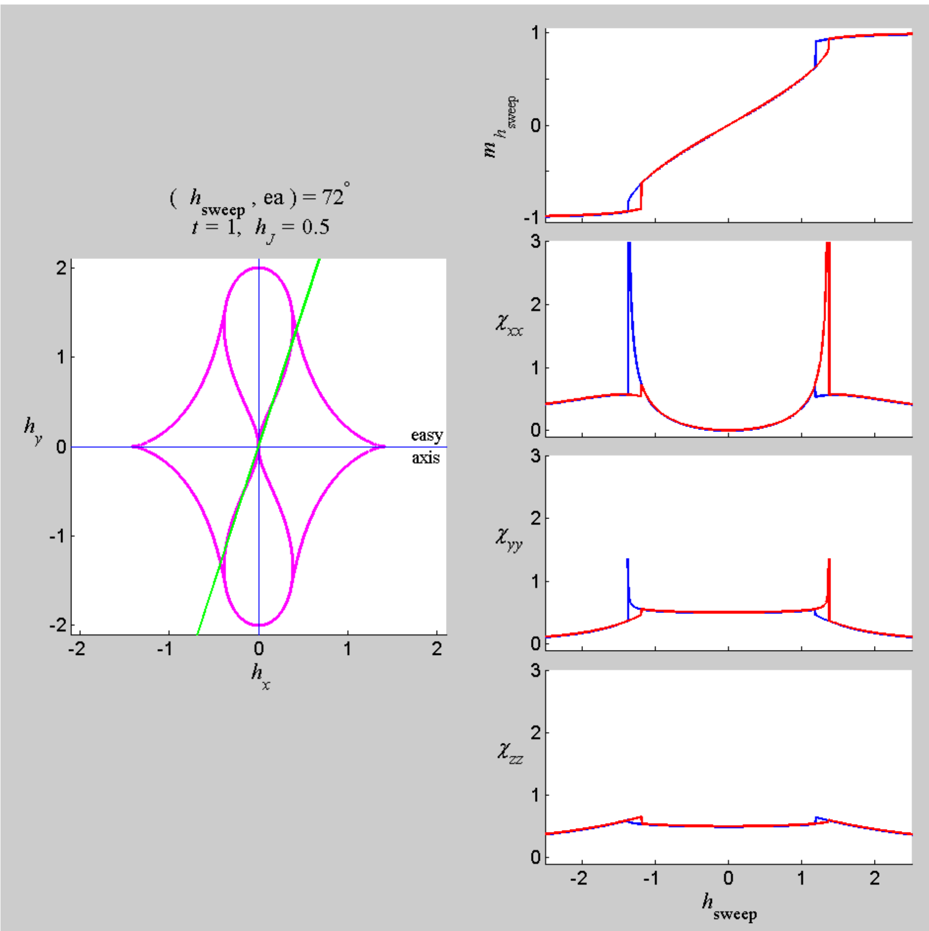

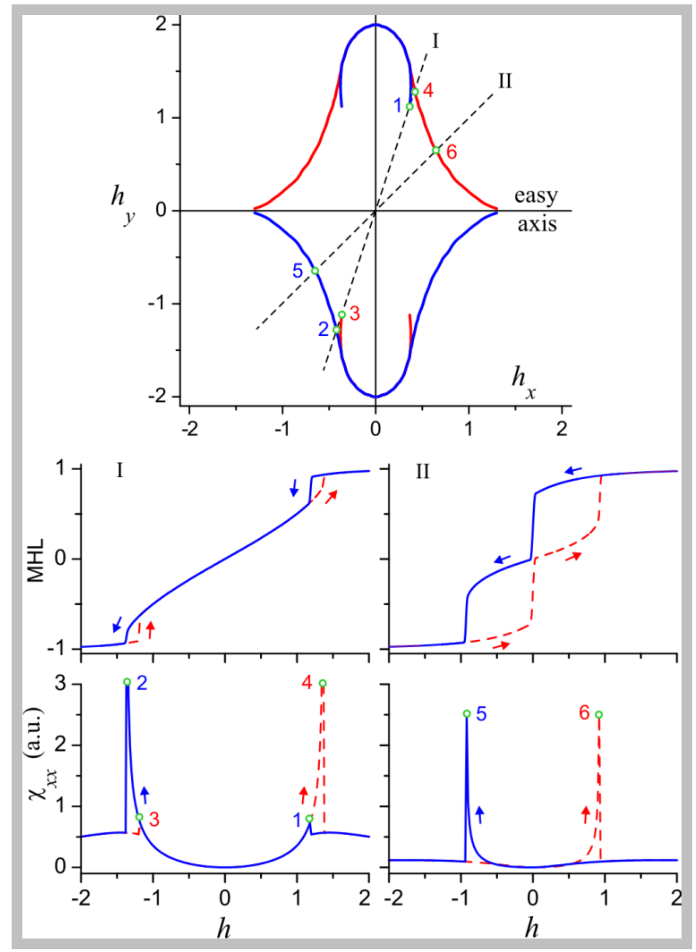

Measurements of the critical curve for a coupled structure

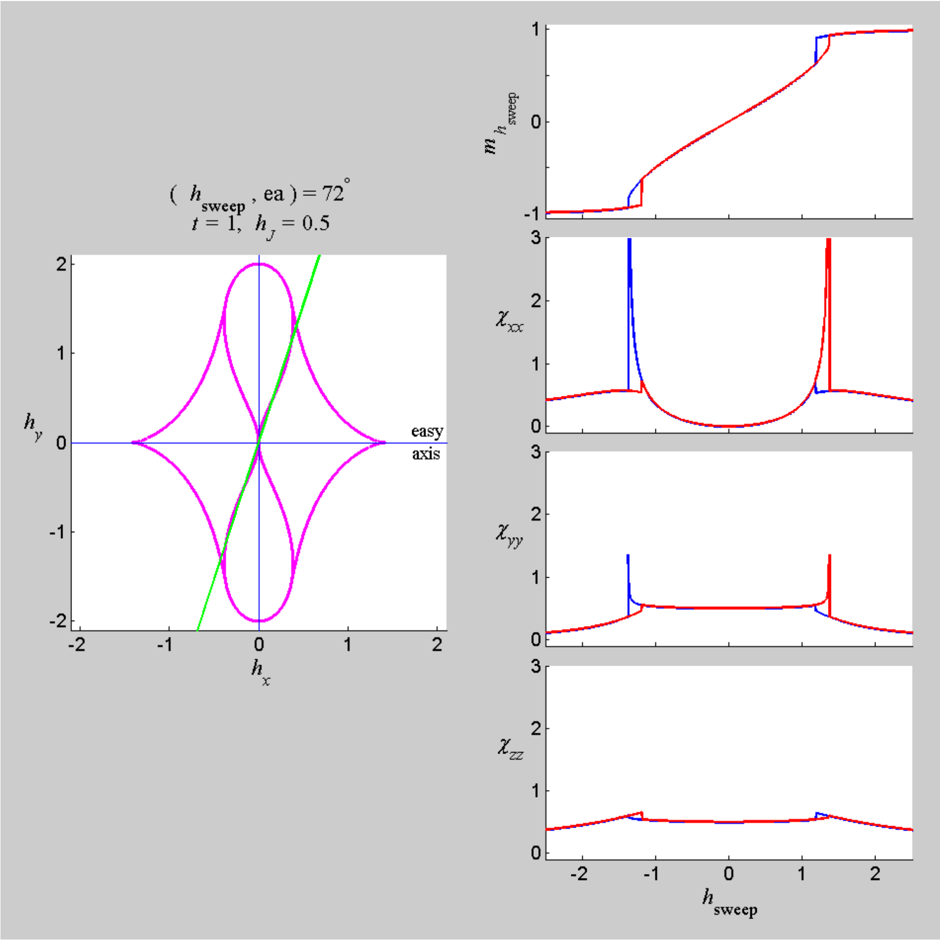

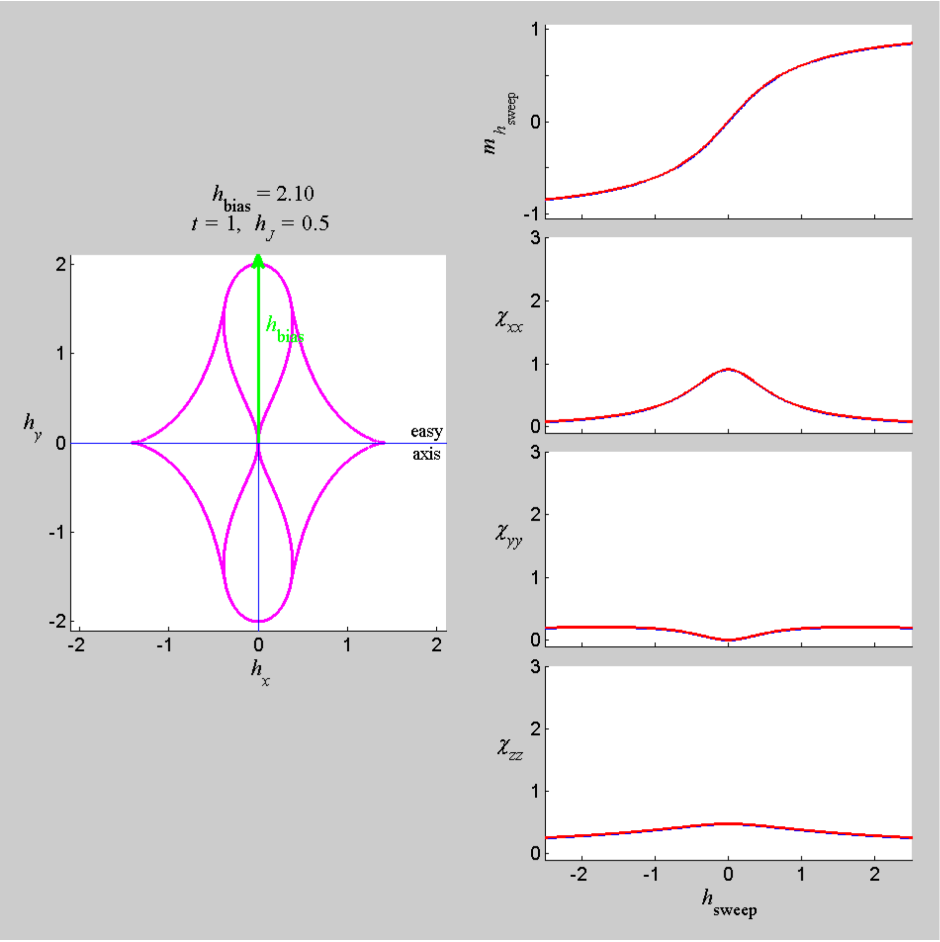

SAF Critical Curves: Theory vs. Experiment

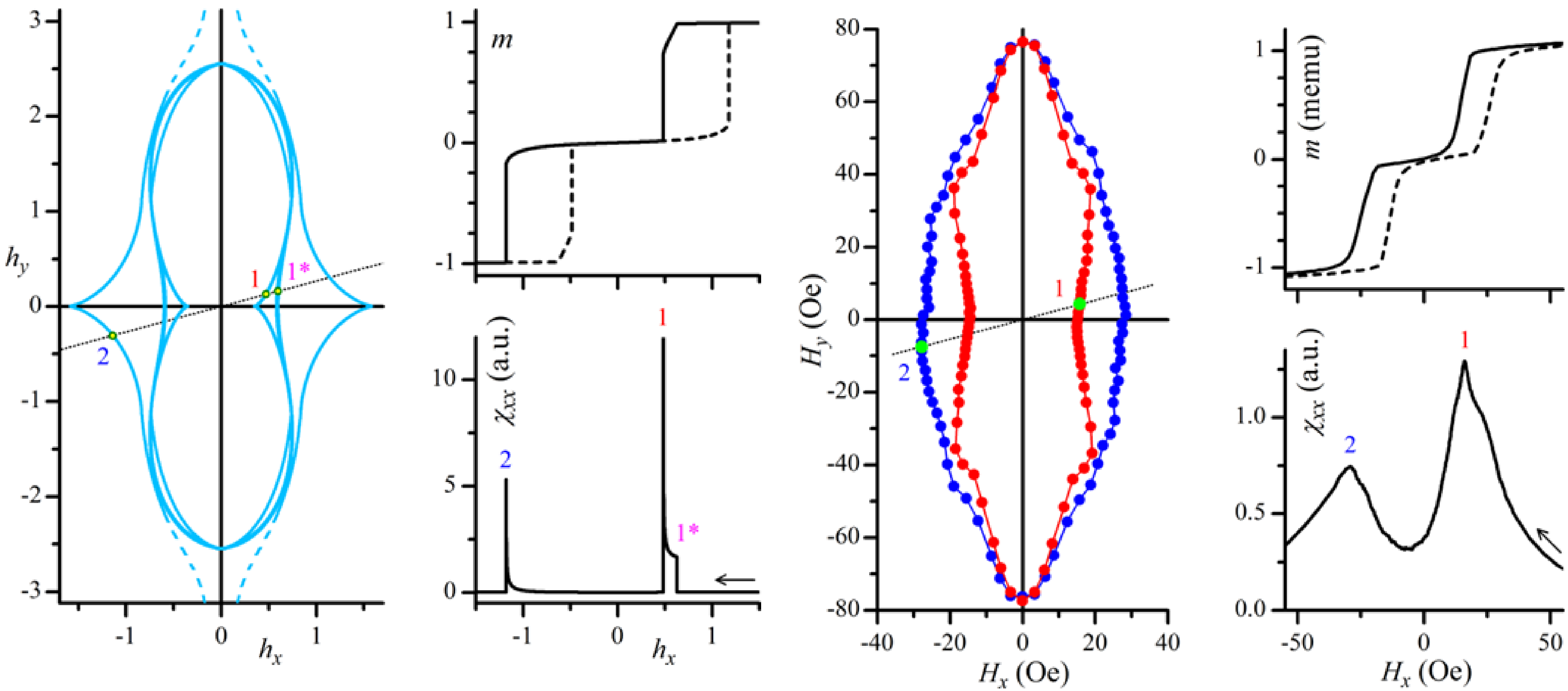

SAF – Dynamical Critical Curves

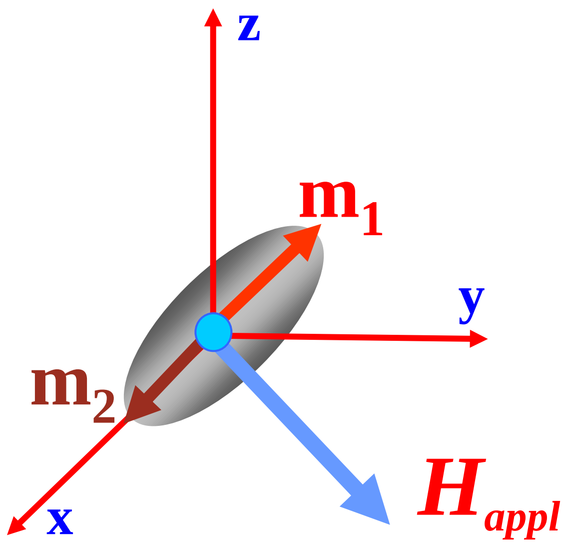

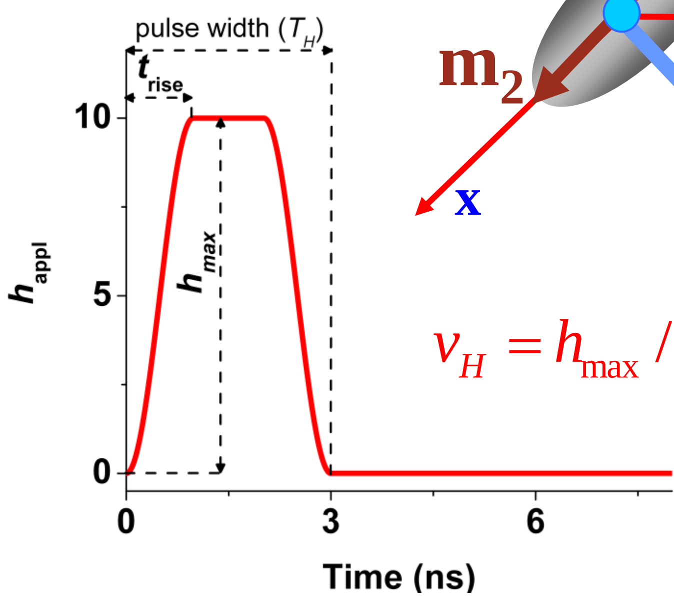

$$v_H = h_{\max} / t_{rise}$$

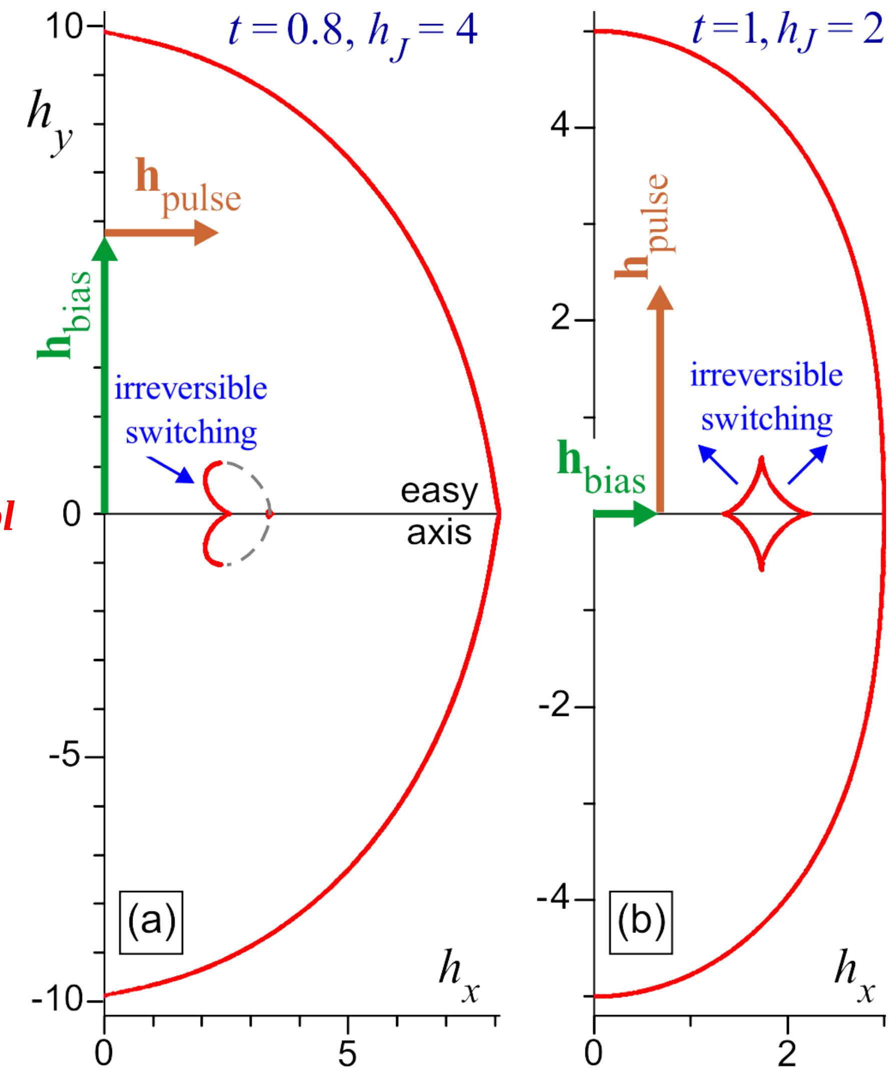

Switching behavior of one SW particle: using field pulses starting from origin.

- M. Bauer *et. al*. PRB 61, 3410, 2000
- H. Pham *et.al*. JAP 97, 10P106, 2005

Switching behavior of SAF: using a bias and a pulse field

Dynamic CC of an asymmetric SAF – sweep rate dependence

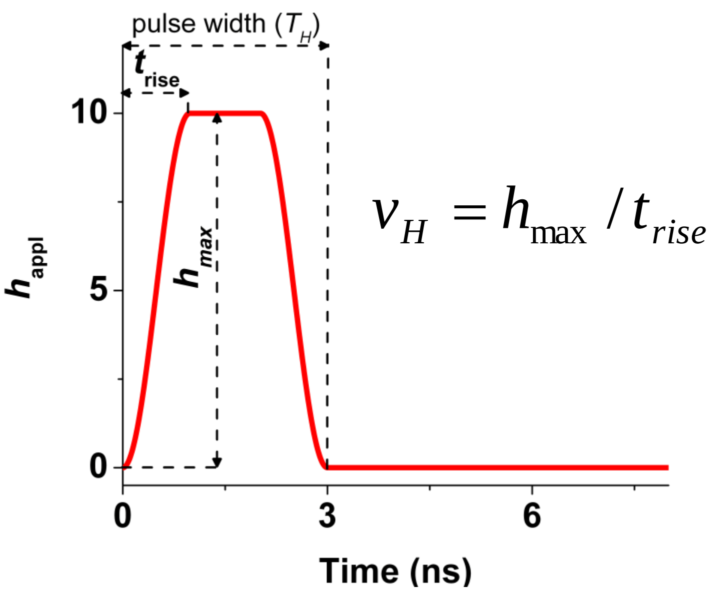

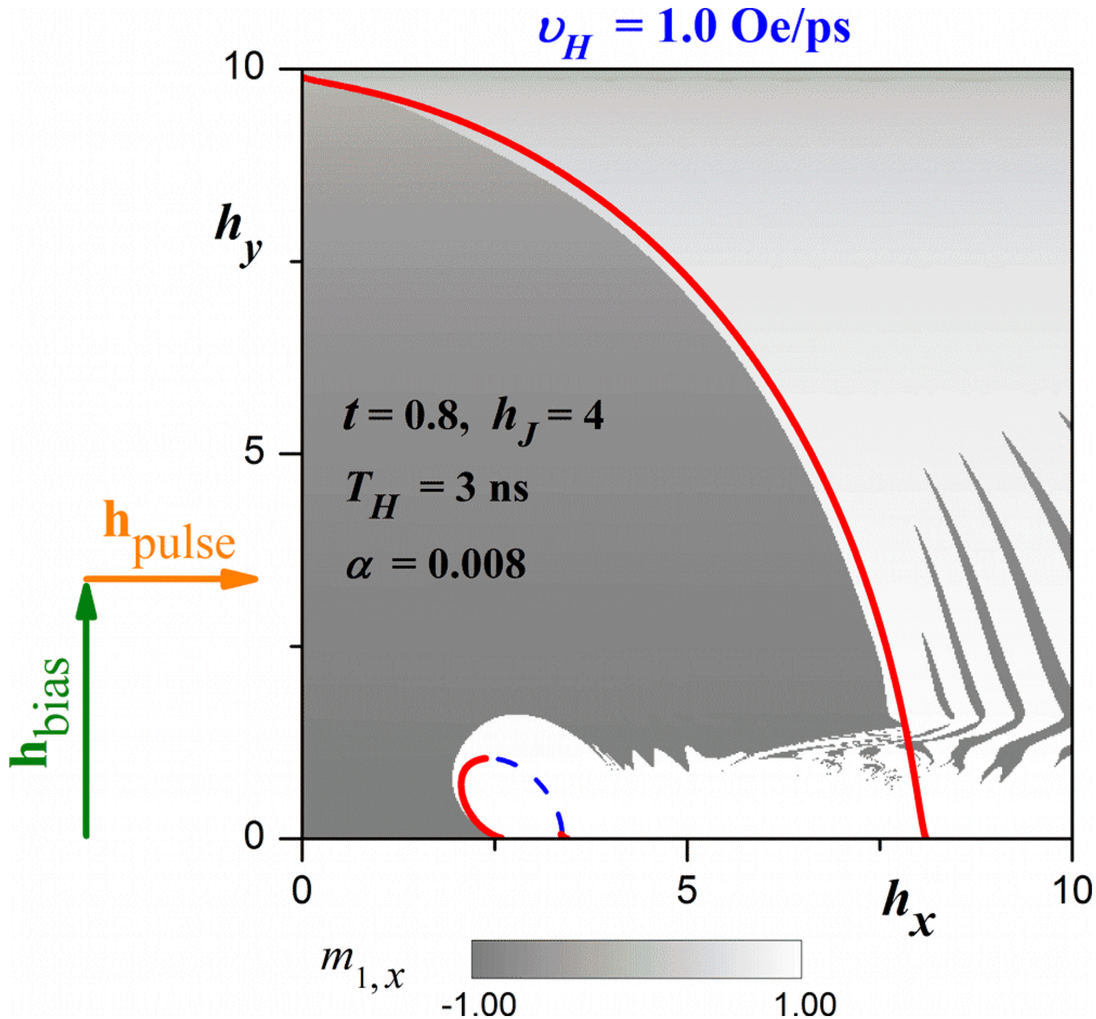

The dynamical CC of a SAF element shows that only a digit or word field, which are the field applied at and with respect to the easy axis in toggle MRAM structure, can switch the magnetization

→ using the static CCs instead of dynamic CCs in characterization of a SAF can lead to inadvertent switching of half-selected memory cells

Dynamic CC of an asymmetric SAF – damping dependence

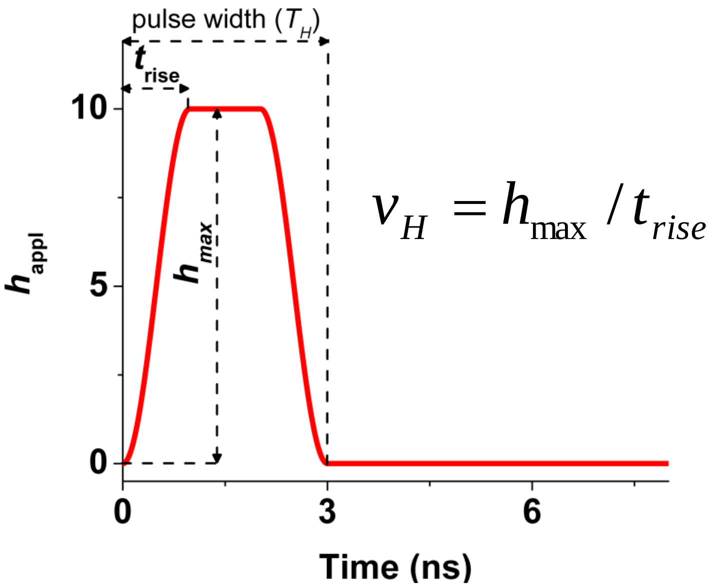

$$v_H = h_{max} / t_{rise}$$

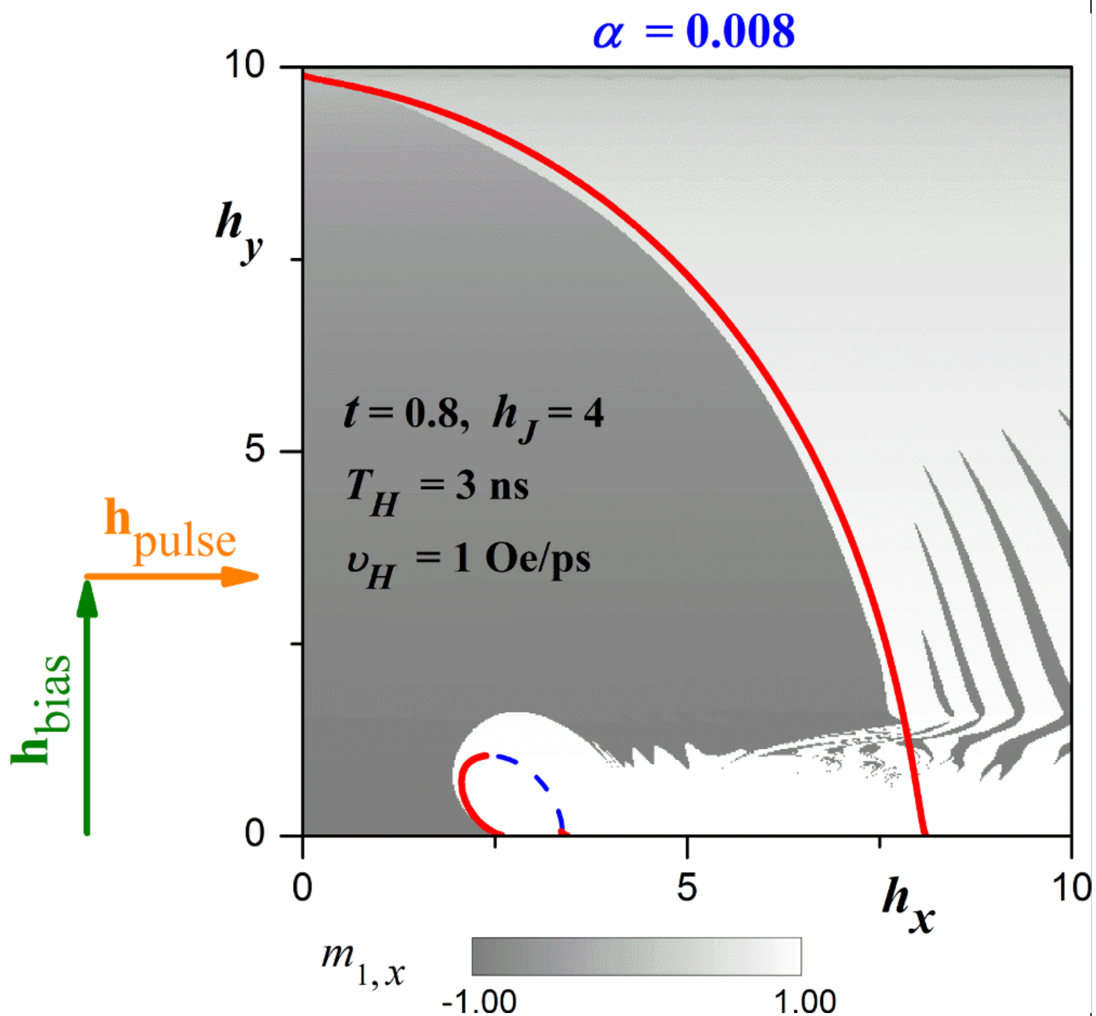

The dynamical CC of a SAF element shows that only a digit or word field, which are the field applied at and with respect to the easy axis in toggle MRAM structure, can switch the magnetization

→ using the static CCs instead of dynamic CCs in characterization of a SAF can lead to inadvertent switching of half-selected memory cells

Dynamic CC of an asymmetric SAF – pulse length dependence

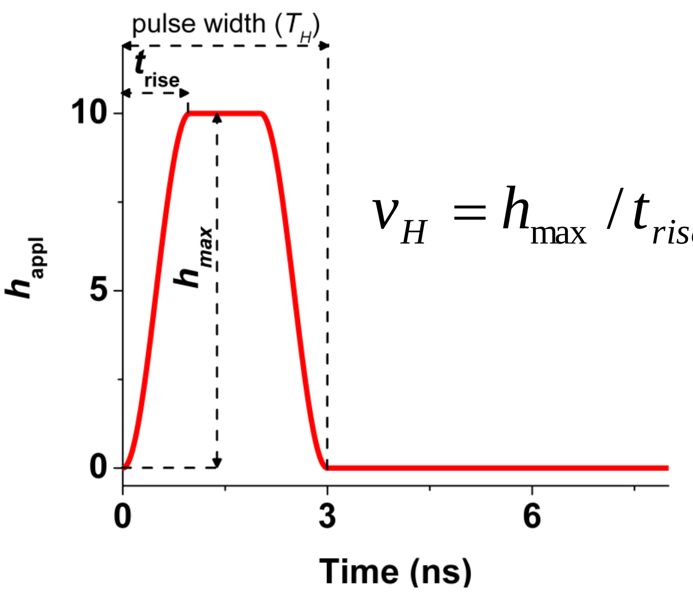

$$v_H = h_{max} / t_{rise}$$

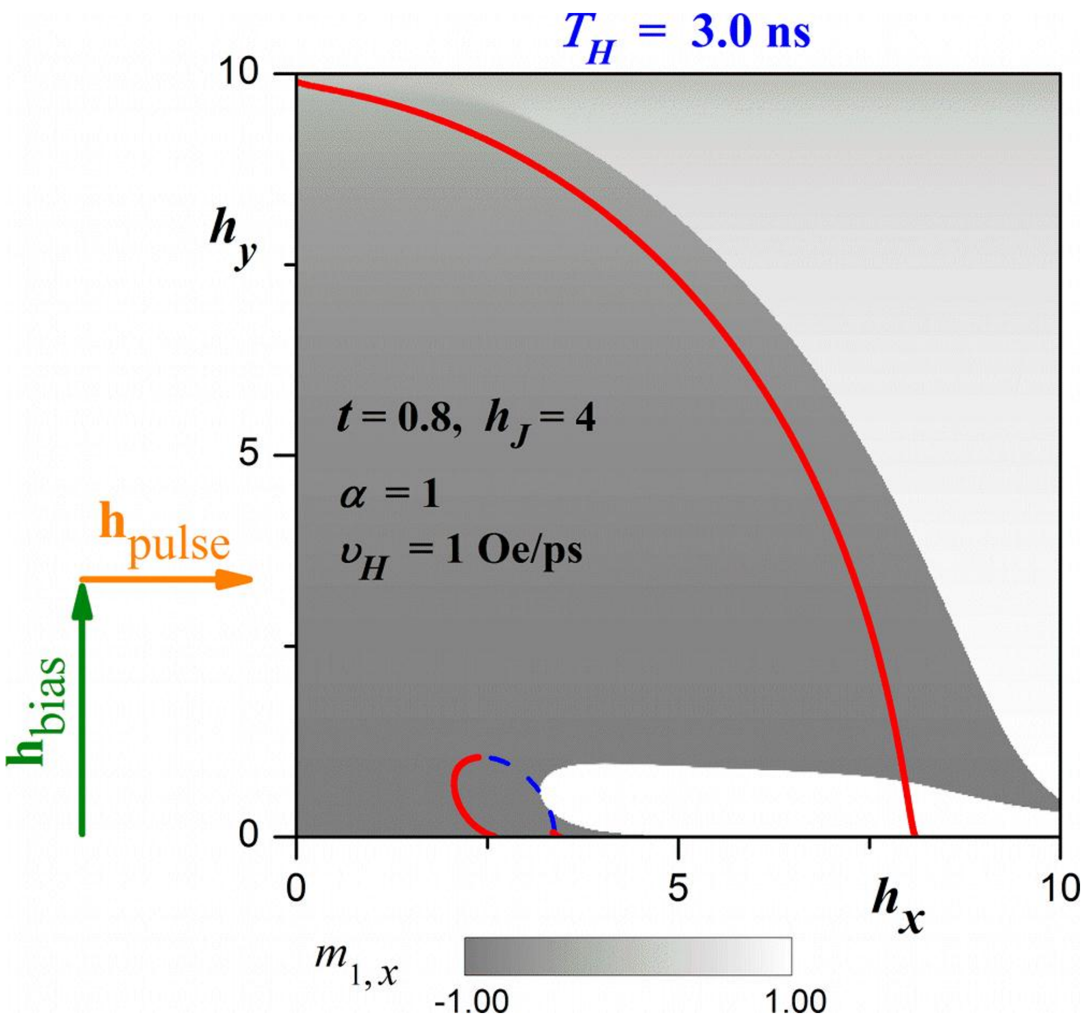

The dynamical CC of a SAF element shows that only a digit or word field, which are the field applied at and with respect to the easy axis in toggle MRAM structure, can switch the magnetization

→ using the static CCs instead of dynamic CCs in characterization of a SAF can lead to inadvertent switching of half-selected memory cells

Dynamic CC of a symmetric SAF – sweep rate dependence

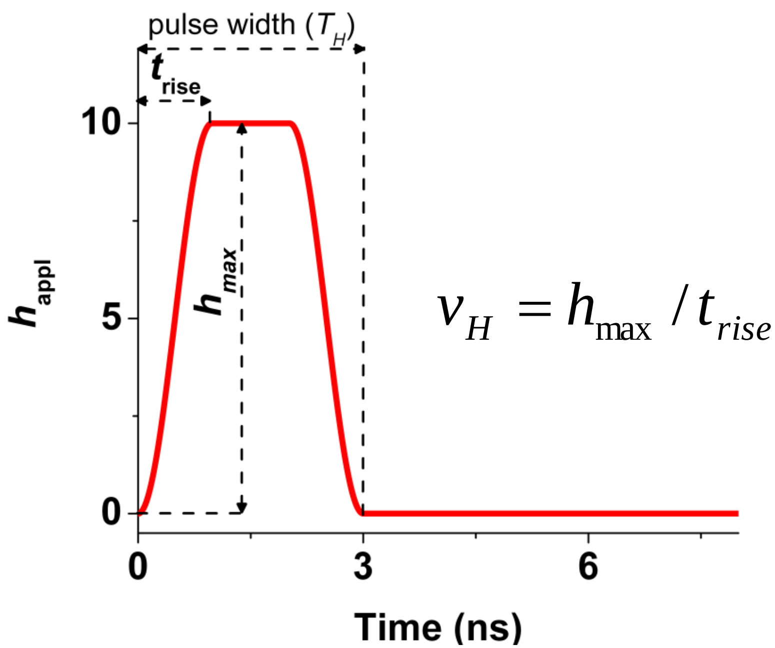

$$v_H = h_{\max} / t_{rise}$$

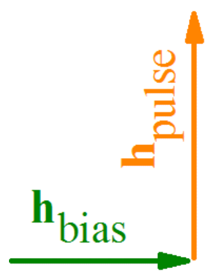

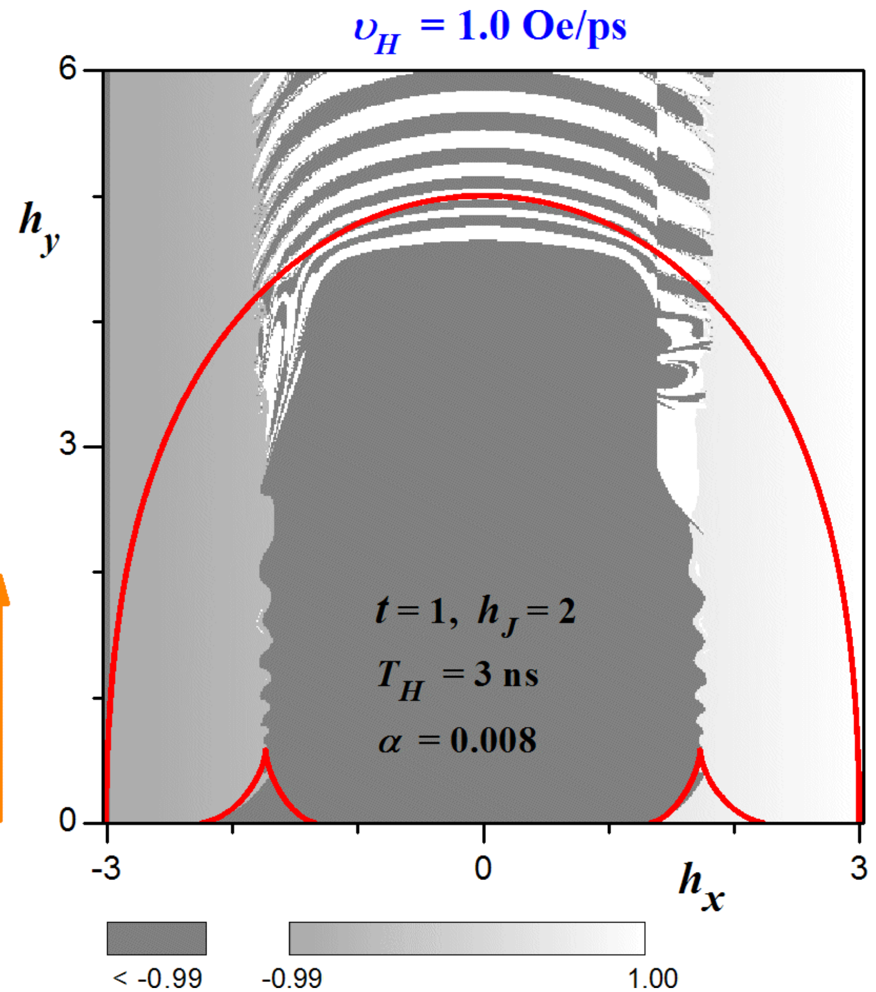

Dynamic critical curve of a synthetic antiferromagnet

Huy Pham,[1] Dorin Cimpoesu,[2,*] Andrei-Valentin Plamadă,[2] Alexandru Stancu,[2] and Leonard Spinu[1,†]

Dynamic CC of a symmetric SAF – damping dependence

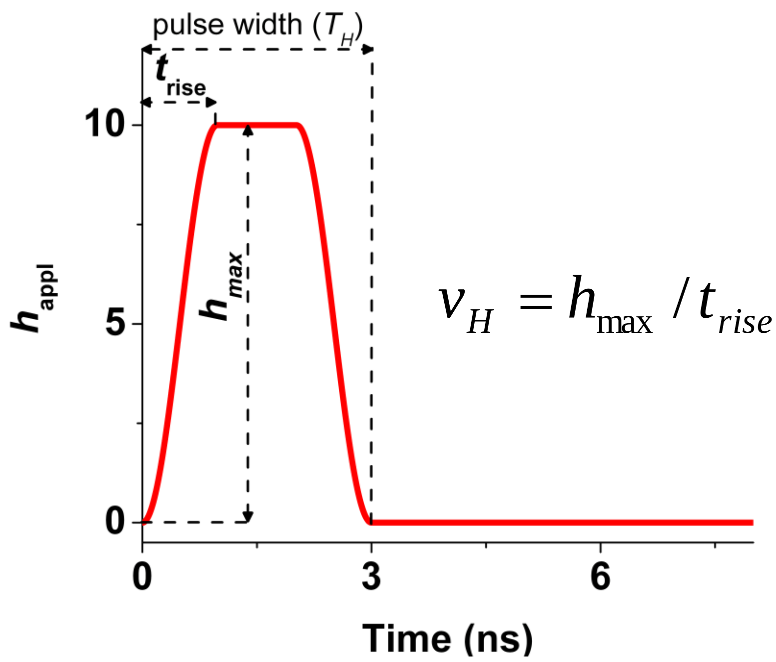

$$v_H = h_{max} / t_{rise}$$

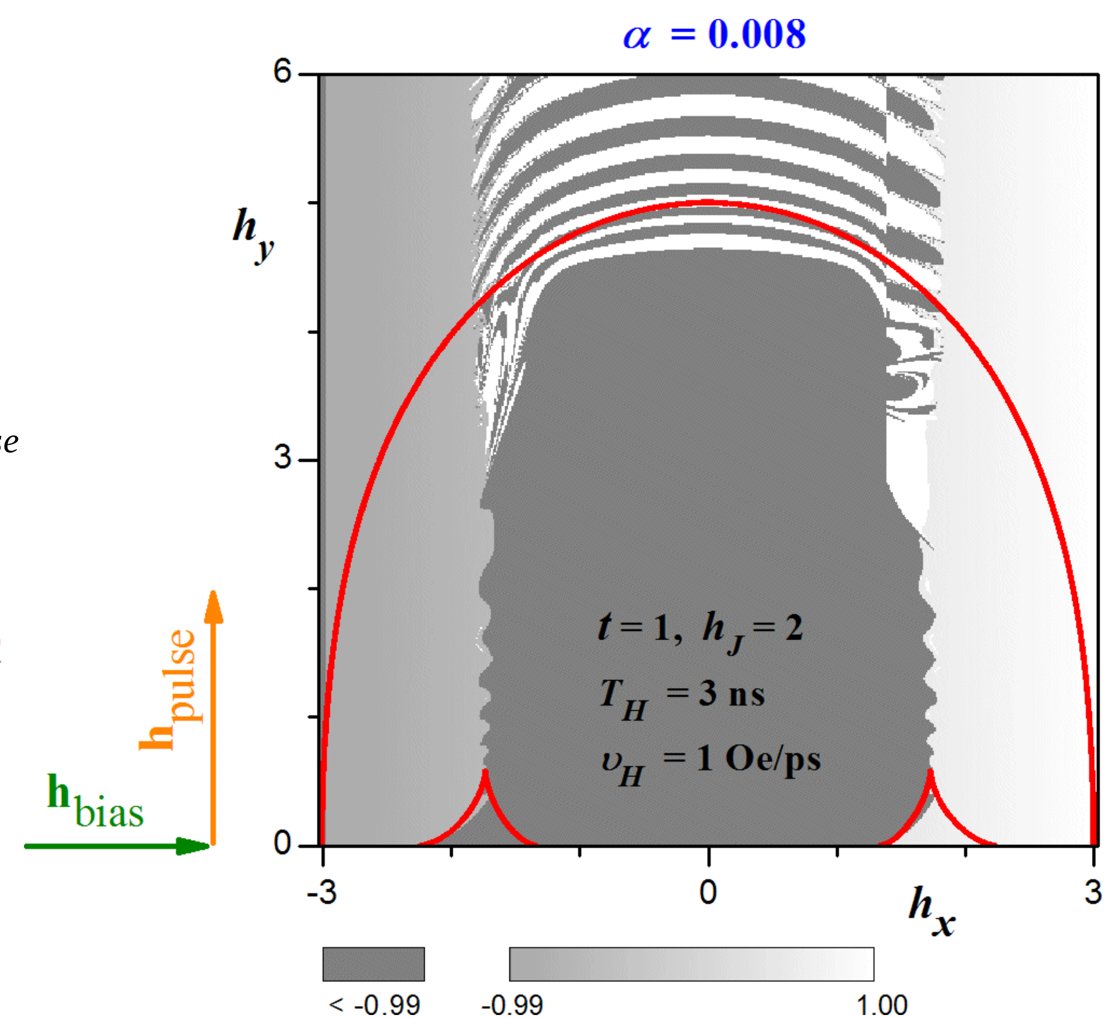

Dynamic critical curve of a synthetic antiferromagnet

Huy Pham,[1] Dorin Cimpoesu,[2,*] Andrei-Valentin Plamadă,[2] Alexandru Stancu,[2] and Leonard Spinu[1,†]

Edmund Clifton Stoner (1899-1968)

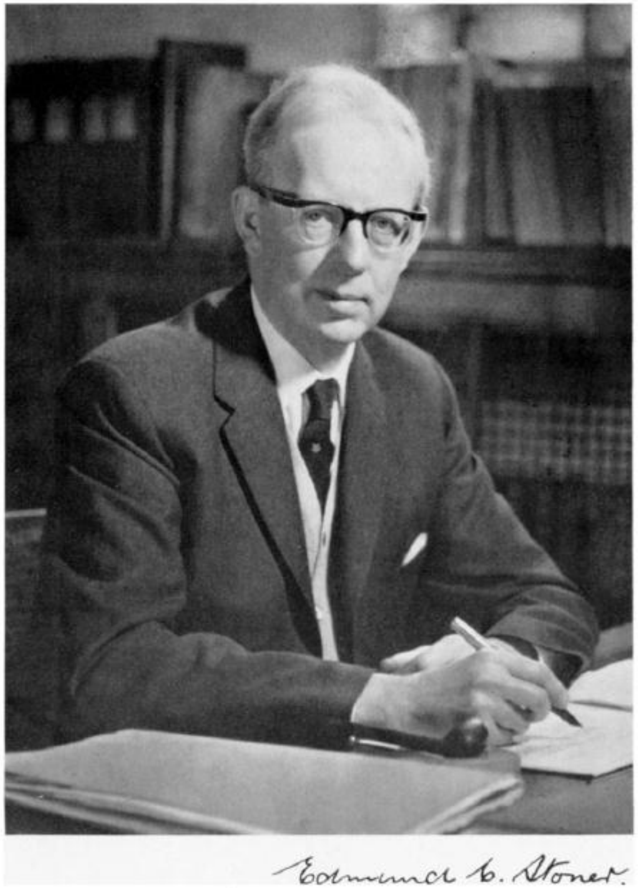

Erich Peter Wohlfarth (1924-1988)

References

- E. C. Stoner and E. P. Wohlfarth, "A mechanism of magnetic hysteresis in heterogeneous alloys," *Phil. Trans. Roy. Soc., vol. A240, pp. 599-644, 1948.*
- J. C. Slonczewski, "Theory of Magnetic Hysteresis in Films and Its Application to Computers," *IBM Research Center Poughkeepsie Research Memorandum R.M.* 003.111.224, 1956.
- G. Bertotti, *Hysteresis in magnetism : for physicists, materials scientists, and engineers. San Diego: Academic Press,* 1998.
- H. Chang, "Analysis of static and quasidynamic behavior of magneostatically coupled thin magnetic films," *IBM J. Res. Dev., vol. 6, pp. 419-429, 1962.*
- H. Fujiwara, S. Y. Wang, and M. Sun, "Magnetization Behavior of Synthetic Antiferromagnet and Toggle-Magnetoresistance Random Access Memory," *Trans. Magn. Soc. Jpn., vol. 4, pp. 121-129, 2004.*